INL/RPT-22-70361

Light Water Reactor Sustainability Program

Application of Margin-Based Methods to Assess System Health

December 2022

U.S. Department of Energy

Office of Nuclear Energy

INL/RPT-22-70361

Application of Margin-Based Methods to Assess System Health

D. Mandelli, C. Wang, V. Agarwal, L. Lin, K. A. Manjunatha

December 2022

Prepared for the
U.S. Department of Energy
Office of Nuclear Energy

SUMMARY

Health management of complex systems such as nuclear power plants is an essential task to guarantee system reliability. This task can be greatly enhanced by constantly monitoring asset status/performances, and processing such data (through anomaly detection, diagnostic, and prognostic computational algorithms) to identify asset degradation trends and faulty states. While such information and data are typically available for many assets, they are not effectively propagated from the asset to the system level in order to identify the most critical assets and prioritize maintenance and surveillance activities. The main reason is driven by the fact that current reliability modeling techniques are inadequate to process such information/data. This is due to the nature of these techniques that are based on the concept of failure probability, and that do not serve an operational context where quantitative asset health information is available. Simply stated, current reliability techniques serve a run-to-failure operational setting and not a predictive maintenance one where the goal is to perform maintenance and surveillance activities only when needed based on asset health. The risk-informed asset management (RIAM) project is focusing on the development of a different kind of reliability modeling techniques designed to adequately serve a predictive operational setting. Such reliability techniques move away from a failure probability mindset to a margin-based mindset. Here, margin is an analytical metric to quantify asset health based only on current and past operational experience of the asset under consideration. Margin-based reliability techniques are able to propagate asset health information to system level, and they can provide analytical importance measures to each asset. This report summarizes a recent activity performed under the Light Water Reactor Sustainability (LWRS) program in collaboration with the plant modernization pathway designed to integrate monitoring data into margin-based reliability models. This integration has been completed for several use cases driven by specific practical applications. Such cross-pathway activity targeted also the direct application of margin-based models on a specific system of an existing nuclear power plant where large amount of historic monitoring data is used to monitor asset and system health.

CONTENTS

SUMMARY iii

ACRONYMS vi

1. INTRODUCTION 1

2. RELIABILITY MODELING IN A PREDICTIVE MAINTENANCE CONTEXT: A MARGIN-BASED APPROACH 3
   2.1 Margin-Based Reliability Modeling 3
   2.2 Integration of ER Data into Margin-Based Reliability Models 5

3. MARGIN ANALYSIS APPLIED TO CWS SYSTEM 8

4. CONCLUSIONS 11

REFERENCES 12

APPENDIX A 14

FIGURES

Figure 1. Graphical overview of the RIAM project. 2
Figure 2. Graphical representation of margin which is based actual asset monitoring data. 4
Figure 3. Margin in a condition-based maintenance context: evolution of asset condition as a function of time and corresponding margin definition. 4
Figure 4. Link between asset health and monitoring systems through failure modes. 6
Figure 5. Margin-based system reliability modeling: provided margin value of each asset, system health and RIM associated with each asset is quantified. 7
Figure 6. Graphical representation of system and health monitoring through margin-based approach. 7
Figure 8. Temporal profile of five selected monitoring variables of the CWS system. 9
Figure 9. Distribution of four selected variables for five different states (healthy and faulty) 9
Figure 11. Temporal profile of system margin for the three considered faulty states. 11

ACRONYMS

AC	alternate current
BE	basic event
CWS	circulating water system
ER	equipment reliability
ET	event tree
FT	fault tree
INL	Idaho National Laboratory
INPO	Institute of Nuclear Power Operations
KNN	k nearest neighbor
LWR	light-water reactor
LWRS	light water reactor sustainability
MCS	minimal cut set
ML	machine learning
MPS	minimal path set
MTTF	mean time to failure
NPP	nuclear power plant
NRC	Nuclear Regulatory Commission
NLP	Natural Language Processing
O&M	operations and management
PHM	prognostic and health management
PWR	pressurized-water reactor
RBD	reliability block diagram
RIAM	risk-informed asset management
RIM	reliability importance measure
RUL	remaining useful life
SR^2ML	Safety, Risk, Reliability Model Library
SSCs	structures, systems, and components

APPLICATION OF MARGIN-BASED METHODS TO ASSESS SYSTEM HEALTH

1. INTRODUCTION

The management of system health and the optimization system resources are essential tasks that guarantees system operability and availability. Currently, these tasks play a major role in many industries such as chemical, aeronautical-aerospace, and automotive (Pecht and Kang, 2019). Nuclear industry is addressing health management and resource optimization by a well-defined maintenance program. The primary objective of a plant maintenance program is to effectively and efficiently maintain plant assets and systems so that plant safety and production are maximized in a manner that is cost effective. Operating nuclear power plants (NPPs) have successfully achieved high levels of safety as indicated by numerous measures such as data and statistics maintained by regulatory authorities (e.g., United States Nuclear Regulatory Commission [U.S. NRC]), industry oversight organizations (e.g., Institute of Nuclear Power Operations [INPO]), and production (as indicated by average plant capacity factors ~90% for more than the past 10 years). However, achieving these levels of performance has come at a high cost in terms of maintenance expenditures. These high expenditures, combined with the implementation of required safety upgrades, as a result of the Fukushima Daiichi accident in Japan, have challenged the economic viability of operating NPPs. Consequently, number of plants have been prematurely shutdown and decommissioned in the past several years due to an inability to compete economically.

Costs associated with health management and optimization can be reduced by employing advanced prognostic and health management (PHM) techniques (Pecht and Kang, 2019). Practically this can be achieved by (a) constantly monitoring asset status and performances, and (b) processing such data (through anomaly detection, diagnostic, and prognostic computational algorithms) to identify asset degradation trends and faulty states. While such health data is typically available for many assets, it is a challenge to propagate health data from the asset to the system level in order to: identify the most critical assets, prioritize maintenance and surveillance activities, and schedule such activities based on available budget constraints.

At a first look, this appears to be a task that can be solved by reliability methods. However, current reliability modeling techniques are inadequate to process such data. This is mainly caused by the intrinsic nature of these techniques which is based on the concept of failure rate/probability, and, because of it, they do not serve an operational context where quantitative asset health information (e.g., monitoring data coupled with anomaly detection, diagnostic, and prognostic methods) is available. Simply stated, current reliability techniques serve a run-to-failure operational setting, where assets are set to operate until they fail, and not a predictive maintenance setting where the goal is to perform maintenance and surveillance activities only when they are needed based on asset health.

The risk-informed asset management (RIAM) project, under the light water reactor sustainability (LWRS) program[1], is focusing on the development of a different kind of reliability modeling techniques designed to adequately serve a predictive operational setting. These novel reliability techniques transition from a classical failure rate/probability mindset to an innovative margin-based mindset. The concept of margin is here used as an analytical metric designed to quantify the health of an asset. A margin is based only on current and past operational experience of the asset under consideration; note that, it is not an approximated integral representation of the past industrywide operational experience as currently

[1] Official LWRS website: https://lwrs.inl.gov/SitePages/Home.aspx

performed by classical reliability models. In addition, margin-based reliability techniques are able to propagate asset health information from the component to system level and provide importance measure to each asset.

A margin-based approach directly addresses the limitations of classical reliability modeling approaches, and it provides a snapshot of system health given available monitoring data. Both reference (Mandelli, 2022) and Appendix A provide a good comparison between classical and margin-based approaches and they provide insights on their targeted decision process. These two different approaches are in fact designed to address different kinds of decisions: classical reliability models well support *static* decisions (e.g., set frequency of periodic maintenance or surveillance operations) based on past operational experience. A margin-based approach directly supports *dynamic* decisions where maintenance operations should be performed only when are necessary based on monitoring data (i.e., a predictive maintenance context). This is due to the fact a margin-based approach transforms the concept of reliability modeling from one that focuses on the probability of failure to one that focuses on assessing how far an asset (or a system) is to an unacceptable level of performance. This transformation has the advantage that it provides a direct link between the asset health evaluation process and standard plant processes used to manage plant performance (e.g., the plant maintenance and budgeting processes) (Xingang, 2021). The transformation also places the question into a more familiar and readily understandable form for plant system engineers and decision makers. The objective of the RIAM project is to develop an integrated health management approach to support plant decision makers in optimizing plant maintenance, testing, and surveillance activities. This optimization will reduce costs and improve plant economics while simultaneously maintaining plant safety and production at the highest levels achievable.

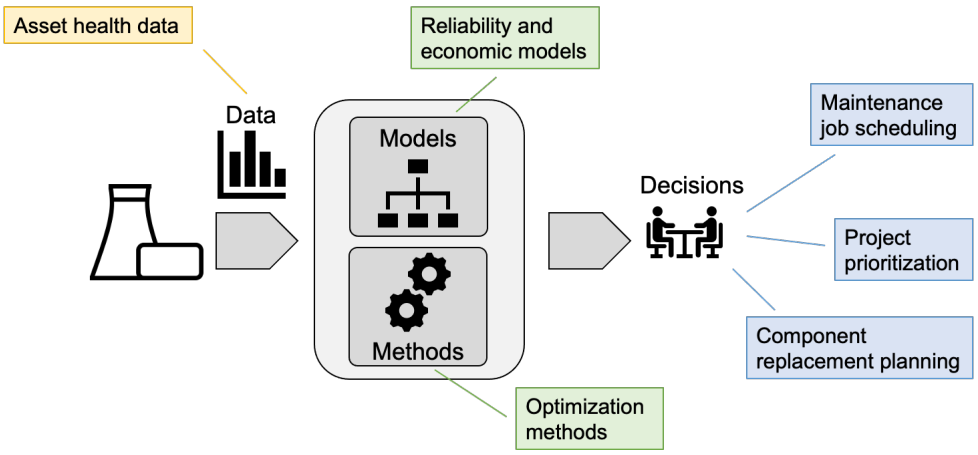

Figure 1. Graphical overview of the RIAM project.

As a notation that we follow throughout this report, we indicate with the term *system* a collection of assets designed to provide a specific function (e.g., provide alternate current [AC] power, or provide high pressure injection during a loss of coolant accident). The term *asset* indicates an element of the system designed to support system function (e.g., a diesel generator, a motor operated valve, or a centrifugal pump). We indicate with the term *component*, a sub element of an asset that is subject to degradation/aging and might require maintenance activity (e.g., a transmission gear of a diesel generator, the drive sleeve of a motor operated valve, or the impeller of a centrifugal pump).

In addition, we indicate with the term *equipment reliability* (ER) data, all data elements that contribute to assess the health of an asset. The data elements can be generated by monitoring systems (i.e., condition-based data) coupled with data analytics methods (e.g., anomaly detection, diagnostic, and prognostic

methods). Data elements that are relevant from a PHM standpoint are also operational tech-spec data (which report limiting conditions for an asset), but also reliability parameters, such as mean time to failure (MTTF), which provide a summary an historical performance of similar assets.

This report presents the most recent activity performed in collaboration between the risk informed systems analysis[2] and plant modernization[3] pathways (which both fall under the LWRS program as well) designed to integrate available monitoring and PHM data into margin-based reliability models. Such activity has been performed on the circulating water system (CWS) of an existing light-water reactor (LWR) where large amount of historic health monitoring has been collected and processed. This report has been structured in two parts: the first one, which is composed of Sections 2 through 4, provides a summary of this activity and the major highlights from the analysis of the CWS system. The second part, located in Appendix A, provides more technical details of this cross-pathway activity in the form of a journal paper which will be submitted shortly after the release of this report.

2. RELIABILITY MODELING IN A PREDICTIVE MAINTENANCE CONTEXT: A MARGIN-BASED APPROACH

2.1 Margin-Based Reliability Modeling

As indicated in Section 1, classical reliability approaches have limitations in terms of integration of plant health data and support decision-making. Condition-based, diagnostic, and prognostic data are in fact not considered in system reliability models to inform system engineers on the most critical components. Currently, the propagation of quantitative health data from the component to the system level is a challenge given the diverse data nature and structure. On the other hand, classical reliability methods (typically based on fault trees [FTs] or reliability block diagrams) can effectively propagate failure data from the component to the system level, but employed failure data (i.e., values of failure rates or failure probabilities) is an approximated integral representation of the past industrywide operational experience, and they neglect the present component health status (e.g., diagnostic and condition-based data) and health projection (when available from prognostic data). In a predictive maintenance context, asset health should be informed solely by that specific component current and historical performance data and, should not be an approximated integral representation of the past industrywide operational experience.

A margin-based reliability modeling (Mandelli, 2022) expands the meaning of the word “reliability” to encompass a broader meaning that better reflects the needs of a system health and asset management decision-making process. Instead of focusing on how likely an event is to occur (in probabilistic terms), we think in terms of how far this event is from occurring. This shift of mindset transforms the concept of reliability from one that focuses on the probability of occurrence to one that focuses on assessing how far away (or close) an asset is to an unacceptable level of performance or failure (see Figure 2).

First of all, note that, in the definition of margin, two data elements are required: the estimated actual health condition of the asset (which can be available from motoring system or from diagnostic methods), and limit conditions that must avoided (which can be available from past operational experience such as monitoring data of similar assets under failure conditions). Note that the margin value of an asset is not static, but it changes with time depending on asset conditions. As an example, if degradation due to usage is observed from monitoring data, then the corresponding asset margin value decreases. Conversely, if a maintenance operation is performed on the same asset (e.g., restoration of bearings of a centrifugal pump), then asset margin value increases.

[2] Official website: https://lwrs.inl.gov/SitePages/Risk-Informed%20Systems%20Analysis.aspx

[3] Official website: https://lwrs.inl.gov/SitePages/Plant%20Modernization.aspx

From Figure 2 note that there is a direct link between margin and decision making (e.g., schedule a maintenance activity). The need of maintenance operation is directly driven by asset margin which is indicator of its health. Figure 2 shows in graphical form how the concept of margin creates a clear bridge between system and data engineers which are essential PHM elements (Pecht and Kang, 2019).

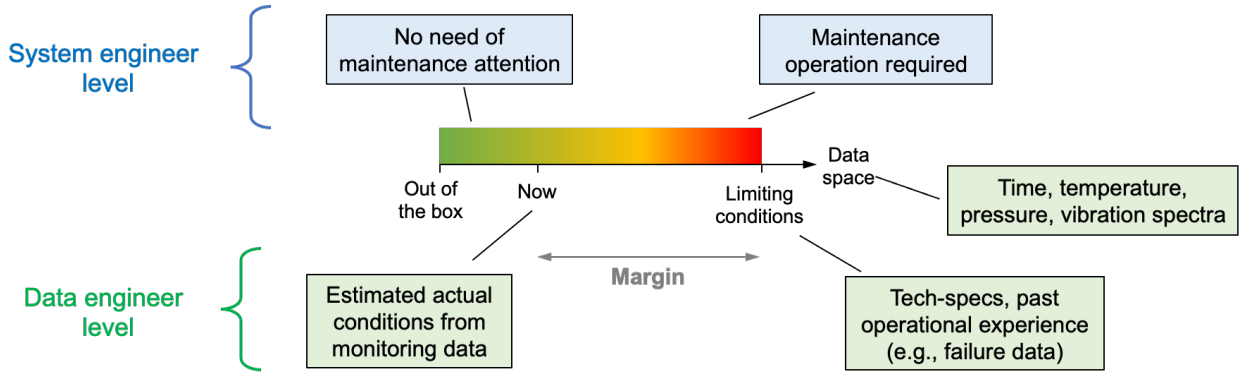

Figure 2. Graphical representation of margin which is based actual asset monitoring data.

More precisely, a margin value M for an asset is defined over the $[0,1]$ interval where $M = 1$ corresponds to a perfectly healthy asset (which requires little or no maintenance attention), while $M = 0$ corresponds to a faulty asset (which requires maintenance attention). Figure 2 provides a glimpse in graphical form of the link between monitoring data and decision making that can be established through a margin mindset: this mindset shift of the concept of reliability (margin based instead of probability based) has the advantage that it provides a direct link between asset health evaluation process and standard plant processes used to manage plant performance (e.g., the plant maintenance operation and budgeting processes). The transformation also places the question into a form that is more familiar and readily understandable to plant system engineers and decision makers.

Note that margin quantification is impacted by the availability of monitoring data and can be defined over heterogenous variables such as pressure, vibration spectra, and time. As an example, when dealing with condition-based data (current and historical data), margin M is defined here as the distance between actual and past conditions (e.g., oil temperature, vibration spectrum) that lead to failure (see Figure 3). Hence, a margin-based modeling provides a unified approach to deal with heterogeneous monitoring data elements. In this work we have focused on numeric ER data; however, a margin-based approach can be integrated with natural language processing methods (Mandelli and Wang, 2022) designed to extract health information form textual data.

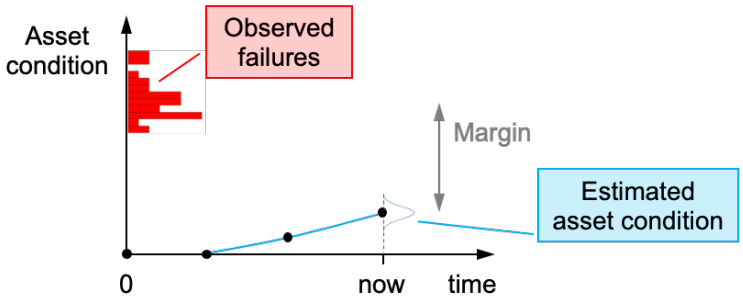

Figure 3. Margin in a condition-based maintenance context: evolution of asset condition as a function of time and corresponding margin definition.

2.2 Integration of ER Data into Margin-Based Reliability Models

As indicated in Section 2.1, the assessment of asset health integrates available data into a unique margin value. The main challenge is that a margin value can be defined over heterogenous variables such as pressure, vibration spectra, and time. In this respect, during this work, we extensively focused on the most critical part of margin-based reliability modeling: the direct integration of asset reliability, monitoring, and condition-based data into the quantification of margin values. We have focused on several practical test cases where, for each test case, a specific data element is translated into margin. The considered test cases are indicated below:

- *Tech-specs data*. Here, limiting conditions (e.g., technical specifications of the considered asset) are normally provided by the manufacturer. When new asset monitoring data becomes available, it is compared to such limiting conditions. By following the definition of margin shown in Figure 2, a margin value can be calculated as the distance between the specified tech-specs limiting condition and current asset monitoring data. As an example, for induction motors, oil viscosity must be below a specified limiting condition to ensure proper motor function. Oil viscosity can significantly change as a function of motor rotation speed. In this context, asset margin can be calculated as the difference between the specified tech-specs limiting condition and the currently measured oil viscosity.
- *Observed reliability parameters*. Current industry-wide available data sets often report asset MTTF values; these values are an integral representation of past operational experience for similar assets operating in similar environmental conditions (e.g., temperature and humidity). Thus, no monitoring data is available, but only knowledge about past operational experience is accessible. This knowledge basically represents the average lifespan of such asset. In this context, asset margin can be calculated as the difference between actual asset age and the estimated MTTF.
- *Data limited to healthy status*. Here we are considering the situation were the available monitoring data for the asset under consideration has been collected exclusively when the asset was in a healthy state; in other terms, data in presence of asset degradation of failure are not available. In this context, the health status of an asset can be established by measuring how actual monitoring data differ (distance wise) from healthy data. In this respect, classical (e.g., kernel density based) and more advanced (e.g., deep-learning based) statistical anomaly detection methods (Hastie et al., 2001), designed to quantify the residual between actual observed data and predicted data, are employed to determine asset margin.
- *Condition-based data*. This situation extends the previously described case where not only data observed under healthy conditions are available but also data observed under faulty conditions. It is here assumed that these two populations differ from each other. In other terms, monitoring data is different under healthy and faulty conditions. We have developed several approaches that employ distance-based and density-based algorithms to quantify asset margin when the aforementioned condition is satisfied. In this situation, machine learning (ML) models (Nassif et al., 2021) (i.e., classifiers) are often developed and tested from healthy and faulty data sets. Asset margin values can be estimated from these models and few test cases have been presented.
- *Prognostic data*. Here, the remaining useful life (RUL) of an asset is estimated using prognostic methods; RUL can provide valuable information about asset failure time. Given the stochastic nature of the phenomena, RUL is typically expressed in terms of probabilistic distribution along the temporal axis. A large number of methods have been developed in the literature to predict RUL for specific assets (Okoh, 2014). For the goal of integrating the RUL into a margin-based reliability model, similar reasoning presented for MTTF is here applied. A margin is defined as the distance between actual time and the predicted RUL. The main differences are that: 1) RUL is estimated

once a degradation mechanism is identified, and 2) RUL is an actual distribution function rather than a point value

So far, a single margin value has been associated with one single asset; it is here implied that monitoring data is designed to assess progression of one single failure mode. In most practical settings, multiple failure modes might be present for a single asset, and the installed monitoring system is designed to detect a subset of these failure modes. In this case, asset failure can be induced by any of the considered failure modes. Figure 4 provides an example where an asset has four identified failure modes and three monitoring systems that can identify one (or more) failure modes. In more detail, each monitoring system can generate one or more observed variables, and the estimation of the margin associated with each failure mode might require observed variables generated by multiple monitoring systems. A margin-based reliability approach is here able to assess a margin value of each of the four failure mode, and to assess asset health based on the four quantified margin values.

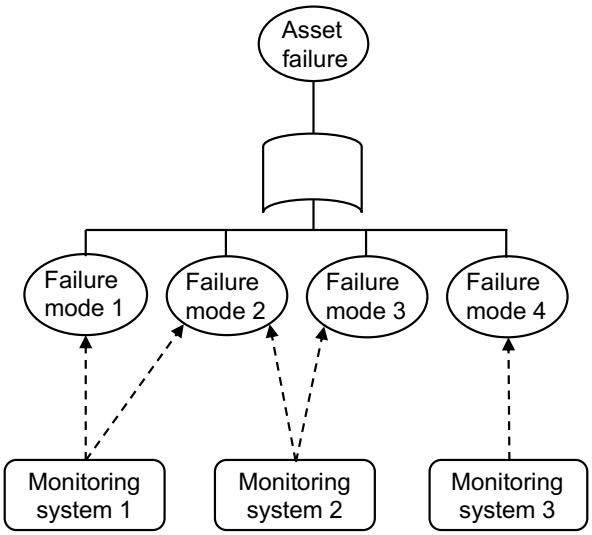

Figure 4. Link between asset health and monitoring systems through failure modes.

As of now we are quantifying health for one single asset; from a decision-making standpoint, this information needs to be put in a system context in order to: (a) understand how asset health contributes to system health and (b) identify which assets are negatively contributing to system health and should be prioritized from a maintenance point of view. Point (b) is redundant when all assets equally contribute to system health and no redundancies or dependencies are present.

For complex systems characterized by several redundancies and dependencies, the task of measuring system health has been completed by developing mathematical methods that propagate margin values from the asset to the system level. Here, we are employing classical system reliability models (e.g., fault trees [FTs] and reliability block diagrams [RBDs]) that are solved using distance-based operations rather than theory based operations (see Figure 5). As indicated in (Mandelli, Wang and Hess, 2022) distance-based operations better fit a predictive maintenance context. The obtained value of system margin is an analytical measure of system health, and it is based solely on all available ER data of each asset.

Importance of each asset is measured using a reliability importance measure (RIM) defined as follows:

$$RIM_{asset} = \frac{\partial\, M_{sys}}{\partial\, M_{asset}} \tag{2}$$

where M_{sys} indicates system margin while M_{asset} represents asset margin. The above RIM definition evaluates the contribution of each asset to system health (see Figure 5) in a derivative form. The RIM associated with each asset can be then used to answer these questions:

- What are the most critical assets?
- What is the added value of operations and management (O&M) funds spent for an asset?

The first question can be simply answered by ordering assets based on their RIM value in descending order. The second question can be answered by considering, for each asset, its RIM value and the amount of funds required to restore asset health.

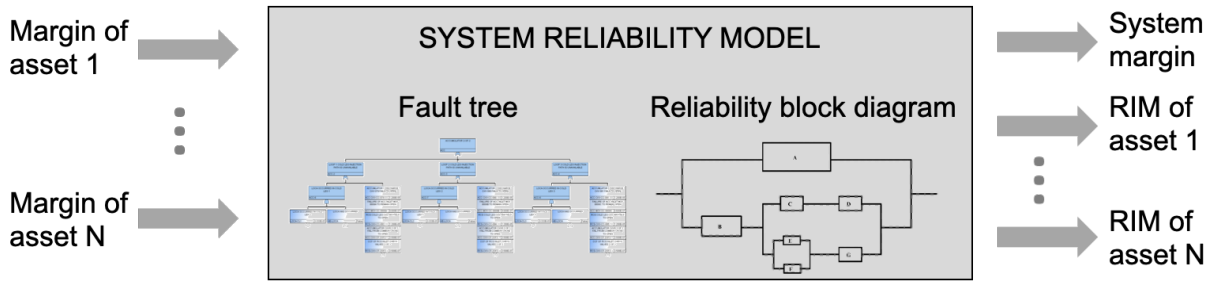

Figure 5. Margin-based system reliability modeling: provided margin value of each asset, system health and RIM associated with each asset is quantified.

Given the basis for the proposed approach, how does it fit with current plant reliability programs? Current power plants typically assess asset health based on collected data and they graphically represent it using a color-coded scheme ranging from green (operational) to red (offline or non-operational). A margin-based reliability approach integrates heterogeneous condition-based data and it quantitively assesses system and asset health using well defined data analytics tools. The essential advantage here is that a direct link between ER data and system health is performed through a set of explainable analytical models.

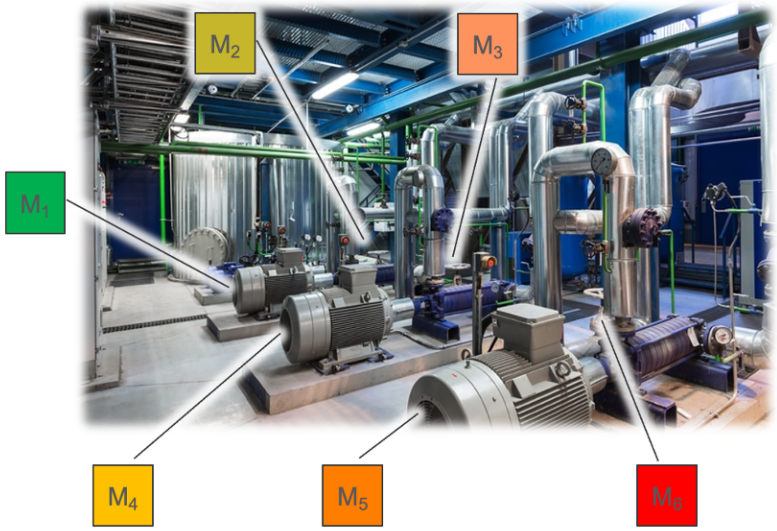

Figure 6. Graphical representation of system and health monitoring through margin-based approach.

3. MARGIN ANALYSIS APPLIED TO CWS SYSTEM

The proposed margin reliability approach has been tested and applied to the analysis of the CWS of an existing PWR plant (see Figure 7). The CWS is an important non-safety-related system. As the heat sink for the main steam turbine and associated auxiliaries, the CWS is designed to maximize steam power cycle efficiency (V. Agarwal, et al. 2021a, V. Agarwal, et al. 2021b). A CWS consists of the following major equipment: vertical motor-driven circulating pumps (each with an associated fixed trash rack and traveling screen at the pump intake to filter out debris and marine life), main condenser, condenser waterbox air removal system, and circulating water sampling system.

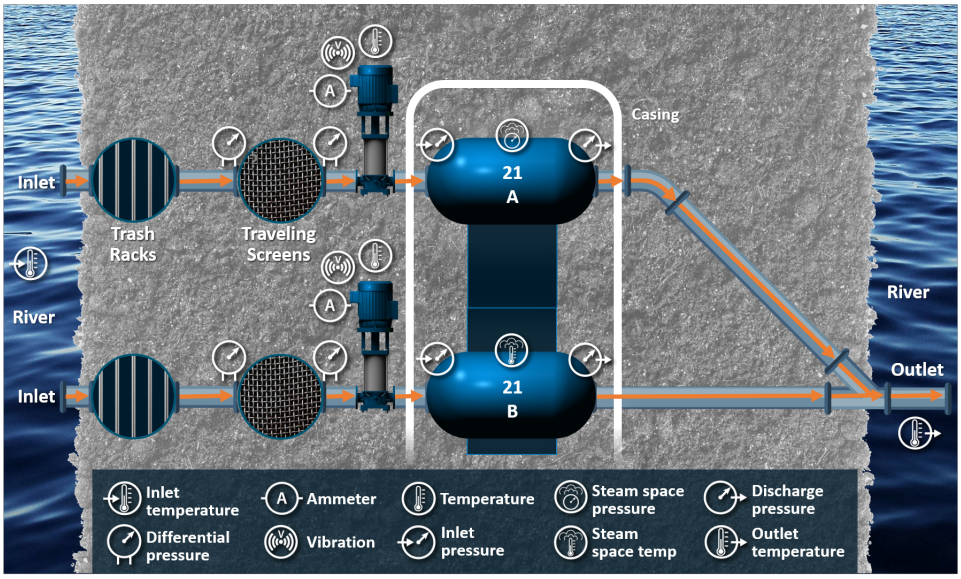

Figure 7. Plant CWS system with sensors and instrumentation.

A large amount of historical data has been collected and employed to track the health profile of the system. This dataset consists of a large number of variables (see Figure 8) of different nature (e.g., temperature, motor current, vibration data). An important observation here is that in some temporal windows, data entries for these monitored variables might be missing due to failure of monitoring system. By performing a separate analysis of the available maintenance logs, it has been possible to identify several faulty states throughout the history of the CWS system. This allowed us to label each data entry for all monitored variables, and identify how distribution of each variable changes from healthy to faulty states. Figure 9 provides in graphical form an initial statistical evaluation of the healthy and faulty populations by considering the box plots for four considered monitoring variables.

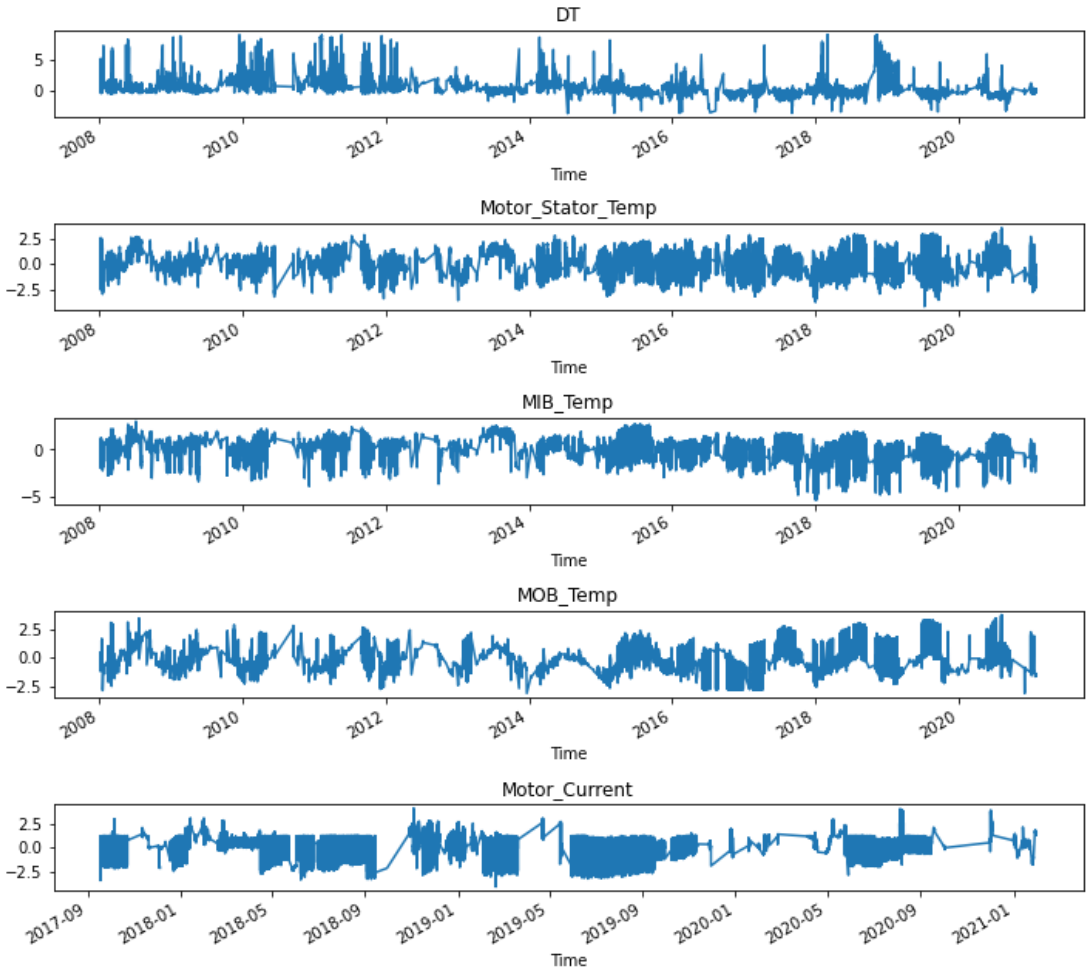

Figure 8. Temporal profile of five selected monitoring variables of the CWS system.

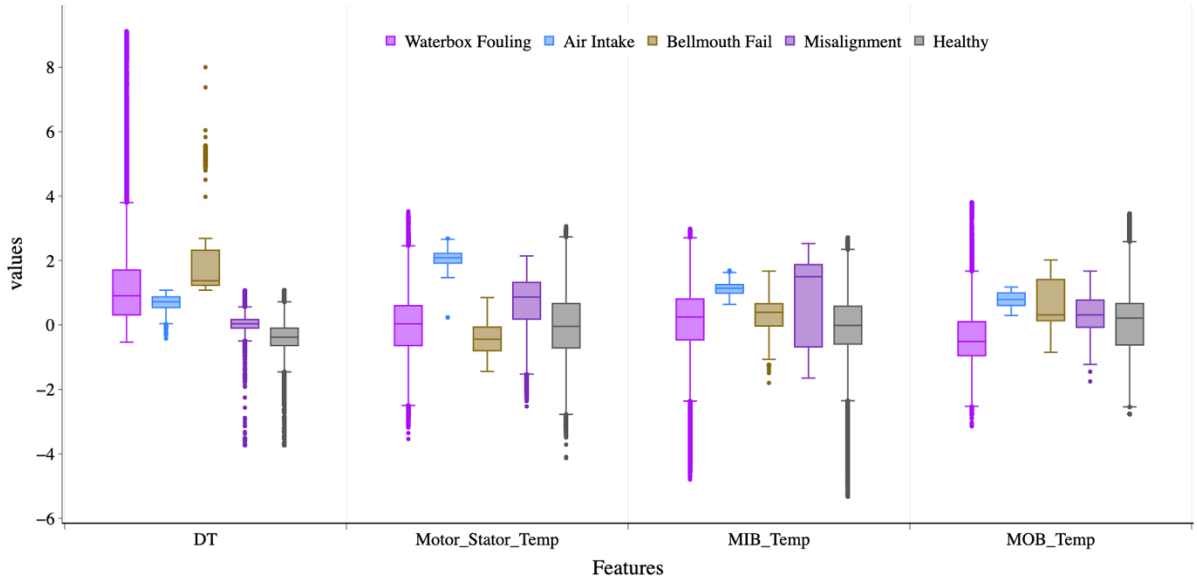

Figure 9. Distribution of four selected variables for five different states (healthy and faulty).

The core of our research activity focused on two tasks: 1) the development of margin-based reliability models based on available monitoring data, and 2) provide an analytical measure of system health through the generated variable *system margin*. Regarding Task 1, we employed both classical statistical analysis tools (e.g., density estimation methods) and ML (i.e., classifier) models to assess the margin associated with a CWS failure mode. An example of margin calculation for a single failure mode of the CWS system is shown in Figure 10; note that even though a margin is point value in the [0,1] interval, it is here the results of the comprehensive analysis of 18 ER data elements of the CWS system (e.g., vibration, temperature).

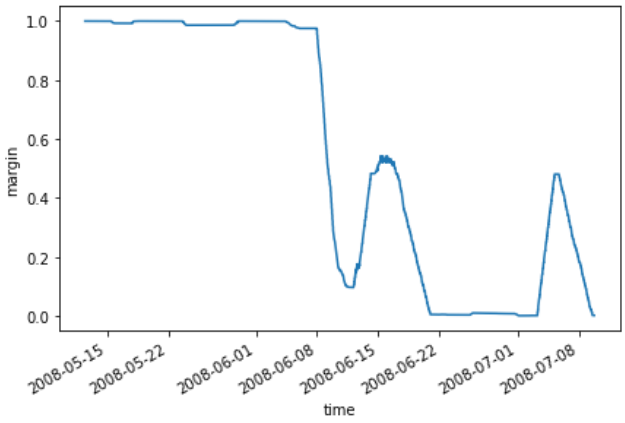

Figure 10. Graphical representation of margin for air-intake during an instance of air intake occurrence using density-based method.

Regarding Task 2, we have proceeded to full integrate all the available ER data of the CWS system and assess the margin associated with each failure mode. Figure 11 provides a representation of the temporal profile of a system margin for three failure modes. The regions highlighted in green in Figure 11 correspond to the times where actual failures occurred. First, note that margin values reach a 0 value when failure occurs. Then, note how margin temporal profiles are characterized by fluctuations and periodic behaviors. While these fluctuations are relatively limited for air intake (bottom plot of Figure 11), they are more pronounced for the other failure modes. This situation is not uncommon when monitoring data under healthy and faulty conditions slightly differ (see also Figure 9). Note that Appendix A provides more technical details about this integration.

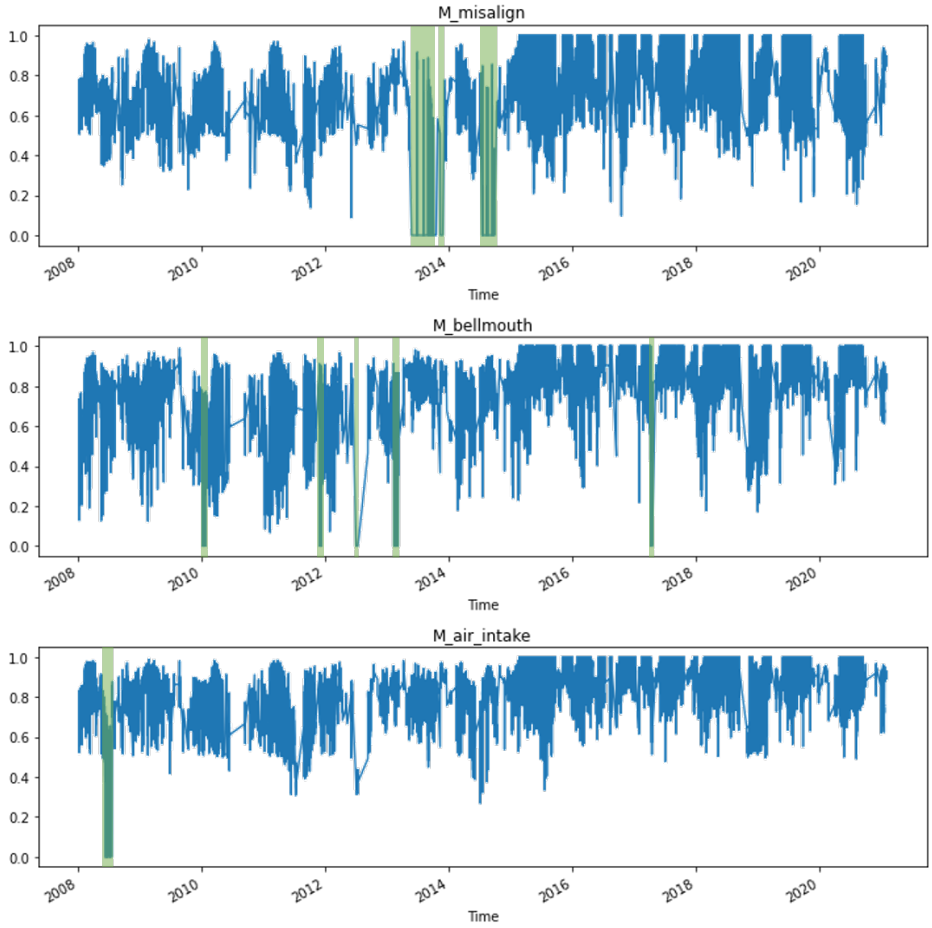

Figure 11. Temporal profile of system margin for the three considered faulty states.

4. CONCLUSIONS

This report has presented a summary of a cross-pathway collaboration under LWRS which was designed to create a robust "bridge" between data and decision in a predictive maintenance context. This "bridge" is structured in three elements (Zio, 2013). The first element focuses on the analysis of available monitoring and PHM data for each single asset and on the quantification of its margin value. Such margin is an analytical measure of asset health, and it is uniquely determined by current and historical performance data of such asset. The second element of this work focuses on the propagation of margin values from the asset to the system/plant level. Here system reliability models (e.g., FTs and reliability block diagrams) are still used to represent functional dependencies and redundancies between assets. The propagation of margin values through FTs or reliability block diagrams is not performed using set theory-based operations but distance-based operations. This allows the analyst to measure not only system health, but also to identify the most critical assets that negatively impact system operation. This is performed by evaluating reliability importance measures for each asset. Lastly, the third element of this work focuses on the prioritization of maintenance activities based on the margin analysis, in particular, on the reliability importance measures obtained for each asset.

A margin-based interpretation of reliability transforms the concept from one that focuses on the probability of occurrence to one that focuses on assessing how far away (or close) an asset is to an unacceptable level of performance or failure. This transformation has the advantage that it provides a direct

link between the asset health evaluation process and standard plant processes used to manage plant performance (e.g., the plant maintenance and budgeting processes). A margin-based approach directly addresses the limitations of classical reliability modeling approaches, and it provides a snapshot of system health given available monitoring data. These two different approaches are designed to address different kind of decisions: classical reliability models support *static* decisions (e.g., set frequency of periodic maintenance or surveillance operations) based on past operational experience. A margin-based approach directly supports *dynamic* decisions where maintenance operations should be performed only when are necessary based on monitoring data (i.e., a predictive maintenance context). Note that the application of these two types of decisions (i.e., *static* and *dynamic*) is dictated by the degradation process under consideration

We have utilized the developed methods to analyze the health performance of the CWS system of an existing U.S. nuclear power station. Starting from a large data set that covered healthy and faulty states associated with the CWS system, we were able to construct a full-margin model for the considered system and monitor system health throughout its history. We have employed both classical statistical analysis and machine learning methods to quantify its margin based on available condition-based data.

REFERENCES

Agarwal, V. et al. (2021a). "Machine Learning and Economic Models to Enable Risk-Informed Condition Based Maintenance of a Nuclear Plant Asset," Idaho National Laboratory Technical Report, INL/EXT-21- 61984, Rev. 0. https://www.osti.gov/servlets/purl/1770866.

Agarwal, V. et al. (2021b). "Scalable Technologies Achieving Risk-Informed Condition-Based Predictive Maintenance Enhancing the Economic Performance of Operating Nuclear Power Plants," Idaho National Laboratory Technical Report, INL/EXT-21-64168.

Hastie, T., R. Tibshirani, J. Friedman (2001). *The Elements of Statistical Learning*. New York: Springer.

Lee, J. C., and N. J. McCormick (2011). *Risk and safety analysis of nuclear systems*. Wiley ed.

Luo Y., W. Zhang, Y. Fan, Y. Han, W. Li, and E. Acheaw (2021). "Analysis of Vibration Characteristics of Centrifugal Pump Mechanical Seal under Wear and Damage Degree," *Shock and Vibration*, 2021. https://doi.org/10.1155/2021/6670741.

Mandelli, D., C. Wang, S. Hess (2022). On the Language Of Reliability: A System Engineer Perspective," Accepted for publication for Nuclear Technology.

Nassif, A. B., M. A. Talib, Q. Nasir, and F. M. Dakalbab (2021). "Machine Learning for Anomaly Detection: A Systematic Review," *IEEE Access*, 9, 78658–78700. https://doi.org/10.1109/ACCESS.2021.3083060.

Okoh, C. et al. (2001). "Overview of Remaining Useful Life Prediction Techniques in Through-Life Engineering Services," Procedia CIRP 16, 158-163.

Pecht, M., M. Kang (2019). Introduction to PHM. Prognostics and Health Management of Electronics: Fundamentals, Machine Learning, and the Internet of Things, IEEE, pp.1-37, doi: 10.1002/9781119515326.ch1.

Rausand, M., A. Barros, and A. Hoyland (2020). *System Reliability Theory: Models, Statistical Methods, and Applications*. Wiley ed.

Xingang, Z., J. Kim, K. Warns, X. Wang, P. Ramuhalli, S. Cetiner, H. G. Kang, and M. Golay (2021). "Prognostics and Health Management in Nuclear Power Plants: An Updated Method-Centric Review

with Special Focus on Data-Driven Methods," *Frontiers in Energy Research*, 9, 696785. https://doi.org/10.3389/fenrg.2021.696785.

Zio, E. (2013). "Prognostics and health management of industrial equipment," in Diagnostics and Prognostics of Engineering systems: Methods and Techniques, S. Kadry, Ed. Hershey, PA, USA: Eng. Sci. Ref., pp. 333–356.

APPENDIX A

Reliability Modeling in a Predictive Maintenance Context: A Margin-Based Approach

D. Mandelli, C. Wang, V. Agarwal, L. Lin, K. A. Manjunatha

Abstract

Current system reliability methods (typically based on fault trees or reliability block diagrams) can effectively propagate reliability data from the asset to the system level in order to identify system critical points. However, employed asset reliability data are an approximated integral representation of the past industrywide operational experience, and they neglect the present asset health status (available, for example, from online monitoring data and diagnostic assessments) and forecasted health projection (when available from prognostic models). Asset health should be informed solely by that specific asset's current and historical performance data and should not be an approximated integral representation of the past industrywide operational experience (as currently performed by system reliability models through Bayesian updating processes). Sensor data, diagnostic assessments, and prognostic assessments are in fact not considered in plant reliability models used to inform system engineers on the most critical assets. In addition, the propagation of quantitative health data from the asset to the system level is a challenge given the diverse nature and structure of health data elements (e.g., vibration spectra, temperature readings, expected failure time). Ideally, in a predictive maintenance context, system reliability models should support decision making by propagating available health information from the asset to the system level in order to provide a quantitative snapshot of system health and identify the most critical assets. This paper is directly addressing these two goals by proposing a different approach for reliability modeling that relies on asset diagnostic and prognostic assessments, along with monitoring data to measure asset health. The propagation of health data from the asset to the system level is performed through fault tree models not in probability terms, but in terms of margin where margin is the "distance" between the present status and an undesired event (e.g., failure or unacceptable performance). Through a cause-effect lens, while classical reliability models target the effect associated with asset performance, a margin-based approach focuses on the cause of an undesired asset performance (i.e., its health). Hence, thinking of reliability in terms of margins implies decision-making based on causal reasoning. We will show how fault tree models can be solved using a margin language and how this process can effectively assist system engineers to identify the most critical assets.

List of acronyms

AC	Alternate Current	MPS	Minimal Path Set
ARIMA	autoregressive integrated moving average	MOB	motor outboard-bearing
BE	Basic Event	MTTF	Mean Time To Failure
CWS	Circulating Water System	NPP	Nuclear Power Plant
DT	Differential temperature	PRA	Probabilistic Risk Assessment
ET	Event Tree	PSEG	Public Service Enterprise Group
ER	Equipment Reliability	PWR	Pressurized Water Reactor
FT	Fault Tree	RIM	Reliability Importance Measure
KooN	K out of N	RUL	Remaining Useful Life
MCS	Minimal Cut Set	TE	Top Event
ML	Machine Learning		
MIB	motor inboard-bearing		

1. Introduction

Current risk approaches are designed to assess and quantify the risk associated with complex systems such as nuclear power plants (NPPs). These approaches are generally based on classical Boolean logic structures such as event-trees (ETs) and fault-trees (FTs). ETs inductively model accident progression using a tree structure with the goal of depicting all possible accident sequences. On the other hand, FTs deductively model the status of a single top event given the Boolean logic status of its basic events (BE). Examples of BEs include failure of specific assets (e.g., centrifugal pumps, or motor operated valves) and failure to perform precise actions by operators or plant personnel (e.g., depressurization of the reactor coolant boundary to allow emergency water injection). The outcome obtained by combining FTs and ETs is the set of minimal cuts sets (MCSs) where each MCS represents a unique combination of BEs that lead to an undesired outcome (e.g., core damage).

The probabilistic evaluation of a MCS is the product of the probability values associated with each BE. A relevant factor here is that the probability value associated with BEs used in the plant models are updated at least every four years (as required by 10CFR50.71 [U.S. CFR, 2010] and the American Society for Mechanical Engineers and American Nuclear Society PRA Standard [ASME and ANS, 2013], which specifies requirements for Probabilistic Risk Assessment [PRA] model upgrades) based on past operational experience through use of a Bayesian statistical process (Siu, 1998). Hence, the probability value of a BE associated with a physical asset (e.g., a centrifugal pump or a motor operated valve) does not reflect in any way its actual condition and performance.

This evidence plays a major role on the application of plant risk models to support risk-informed decisions. In particular, to reduce operation and maintenance costs, existing NPPs are moving from corrective and periodic maintenance to predictive maintenance strategies (Agarwal, V. et al. 2021a, Agarwal, V. et al. 2021b). While corrective maintenance is performed only when the asset fails (with high costs due to asset replacement and unexpected system and plant unavailability, e.g., loss of generation), periodic maintenance is performed at specific time intervals based on reliability factors and past operational experience (with high costs due to continuous maintenance operations that may not be warranted). The transition from periodic or corrective maintenance to predictive maintenance is designed so that maintenance occurs only when the asset requires it (i.e., before its imminent failure). This guarantees that asset availability is maximized and that maintenance costs are minimized. However, these benefits cannot be achieved with actual reliability modeling methods and currently employed reliability data. These benefits can be achieved by employing asset monitoring sensors, automated data acquisition systems, data analysis methods, and improved decision processes. When combined together, they can provide precise information about health of an asset, track its degradation trends, and provide information of its expected failure time.

With such information, maintenance operations can be scheduled and performed for each asset only when needed.

This dynamic context of predictive maintenance operations requires new methods to analyze data, propagate asset health information from the asset to the system level, and optimize plant resources. This paper provides an alternative reliability approach designed for a predictive maintenance context which creates a direct link between monitoring data and decisions. Rather than thinking of reliability in terms of system/asset probability of failure, we are proposing a different reliability mindset based on the concept of margin (Mandelli, 2022). Asset health is quantified by determining its margin, which is based on the asset's current and historical monitoring data. Margin values of the monitored asset are then propagated through system reliability models (e.g., FTs or reliability block diagrams) to identify the assets that are more critical to guarantee system operation.

Section 2 provides a summary of the margin-based reliability modeling (see ref. [Mandelli, 2022] for a more complete description of the approach) while Section 3 provides a detailed description of the integration of equipment reliability (ER) data. ER data includes all possible data elements that are employed to assess asset health such as condition based, anomaly detection, diagnostic, and prognostic data. Section 3 provides practical examples on how ER data is employed to generate a margin value for a specific set of use cases. Section 4 describes a more concrete application of the margin-based reliability modeling for the circulating water system (CWS) of an existing pressurized water reactor (PWR). Lastly, Section 5 provides insights about the use of margin modeling to support decision-making in predictive maintenance contexts which are dynamic in nature.

As a notation that we follow throughout the paper, we indicate with the term *system* a collection of assets designed to provide a specific function (e.g., provide alternate current power, or provide high pressure injection during a loss of coolant accident). The term *asset* indicates an element of the system designed to support system function (e.g., a diesel generator, a motor operated valve, or a centrifugal pump). A *component* denotes a sub element of an asset that is subject to degradation/aging and might require maintenance (e.g., a transmission gear in a diesel generator, the drive sleeve of a motor operated valve, or the impeller of a centrifugal pump) in order to guarantee asset operation.

2. Margin Analysis

Reference (Mandelli, 2022) expands the meaning of the word "reliability" to encompass a broader meaning that better reflects the needs of a system health and asset management decision-making process. Rather than focusing on how likely an event is to occur (in probabilistic terms), we think in terms of how far this event is from occurring. This new interpretation of reliability transforms the concept from one that focuses on the probability of occurrence to one that focuses on assessing how far away (or close) an asset is to an unacceptable level of performance or failure (see Figure 1). Note that two data elements are required: the estimated actual health condition of the asset (which can be available from motoring system or from diagnostic methods), and limit conditions that must avoided (which can be available from past operational experience such as monitoring data of similar assets under failure conditions).

A margin value M for an asset is defined over the $[0,1]$ interval where $M = 1$ corresponds to a perfectly healthy asset (which requires minimal to no maintenance attention), while $M = 0$ corresponds to a faulty asset (which requires maintenance attention). Figure 1 provides a glimpse in graphical form of the link between monitoring data and decision making that can be established through a margin mindset.

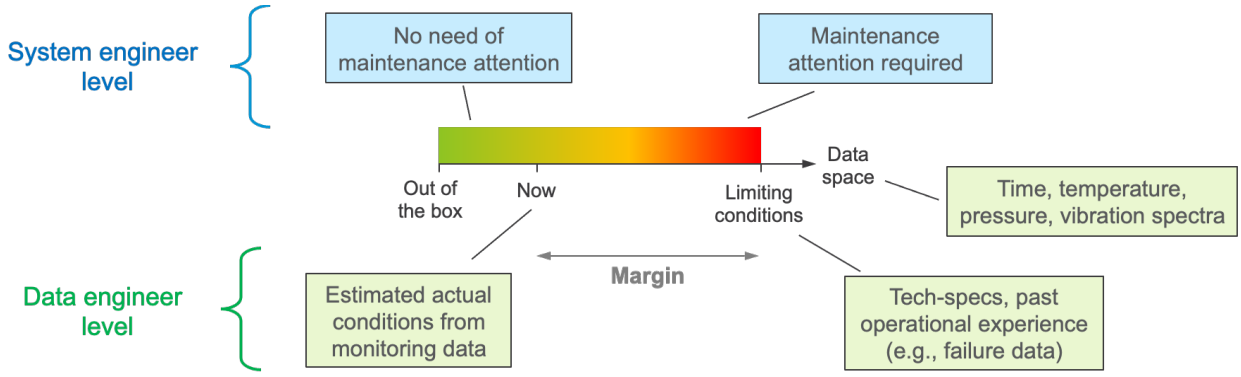

Figure 1. Graphical representation of margin which is based actual asset monitoring data.

Note that margin quantification is impacted by the availability of monitoring data and can be defined over heterogenous variables such as pressure, vibration spectra, and time. As an example, when dealing with condition-based monitoring data (current and archived data), margin M is defined here as the distance between actual and past conditions (e.g., oil temperature, vibration spectrum) that lead to failure (see Figure 2). Hence, a margin-based modeling provides a unified approach to deal with heterogeneous monitoring data elements.

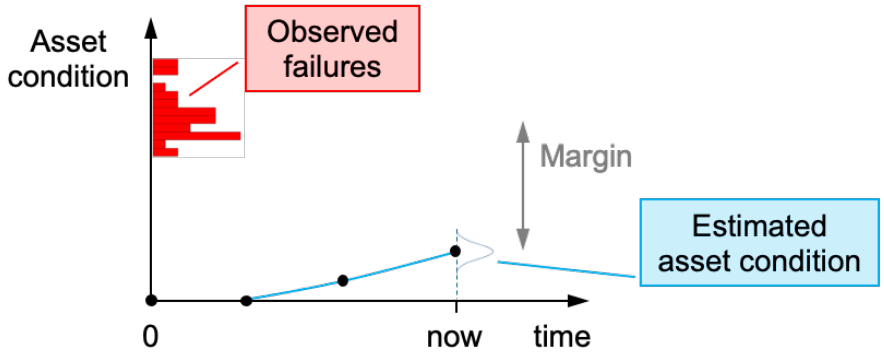

Figure 2. Margin in an online monitoring context: evolution of an asset condition as a function of time and margin estimation.

Note that the margin value of an asset is not static, but changes with time depending on asset conditions. As an example, if degradation due to usage is observed from monitoring data, then the corresponding asset margin value decreases. Conversely, if a maintenance operation is performed on the same asset (e.g., restoration of bearings of a centrifugal pump), then asset margin value increases.

This mindset shift behind the concept of reliability (margin based instead of probability based) has the advantage that it provides a direct link between asset health evaluation process and standard plant processes used to manage plant performance (e.g., the plant maintenance operation and budgeting processes). The transformation also places the question into a form that is more familiar and readily understandable to plant system engineers and decision makers.

So far, margin has been defined for one single asset; the next step is to quantify system margin value provided the margin value of its assets. The propagation of margin values from the asset level to the system level is performed through classical reliability models such as fault trees or reliability block diagrams (Lee, 2011) which are solved using different rule sets (Mandelli, 2022) instead of set theory-based operations.

In this respect, margin-based operators for assets in a series (OR operator) and parallel (AND operator) configurations need to be defined. As an example, let's consider now two assets (A and B). The margin M of both assets can be visualized in a 2D space, as shown in Figure 3. Starting with brand-new assets (i.e., $M_A, M_B = 1$), aging/degradation that affects both is represented by the blue line of Figure 3, which parametrically represents the combination of both margins $M_A(t)$ and $M_B(t)$ at a point in time t. Note that if no maintenance (whether preventive or corrective) was ever performed on either asset, this path would move from the coordinates $(1,1)$ to the coordinates $(0,0)$, where both assets are considered failed. Hence, the point of coordinate $(0,0)$ in Figure 3 represents the event "A AND B." Similarly, when the blue line reaches the x or the y axis of Figure 3 (characterized by $M_B = 0$ and $M_A = 0$ respectively), either asset A or B has failed. Hence, the points in Figure 3 characterized by either $M_B = 0$ or $M_A = 0$ represent the event "A OR B."

Now we can calculate the margin M for the AND and OR events described above. This is accomplished by following the definition of margin: by measuring the distance between the actual condition of assets A and B and the conditions identified by the event under consideration (e.g., the occurrence of both or either event). Margin for $A\ AND\ B$ can be calculated as the distance between current point of coordinates (M_A, M_B) to the point $(0,0)$. Margin for $A\ OR\ B$ is the minimum distance current point of coordinates (M_A, M_B) to the x or the y axis of Figure 3 (where $M_B = 0$ and $M_A = 0$ respectively). In mathematical form:

$$M(A\ AND\ B) = dist[(M_A, M_B), (0,0)] \quad (1)$$

$$M(A\ OR\ B) = min(M_A, M_B) \quad (2)$$

where the function $dist[.,.]$ indicates the metric designed to calculate the distance between two points in an Euclidean space (e.g., if Euclidean distance is employed, then $M(A\ AND\ B) = \sqrt{M_A^2 + M_B^2}$). Reference (Mandelli, 2022) provides a set of considerations about the choice of the distance metric $dist[.,.]$ to be employed. In summary, Euclidean and Manhattan distance metrics represent lower and upper bounds for $M(A\ AND\ B)$, i.e., $\sqrt{M_A^2 + M_B^2} \leq M(A\ AND\ B) \leq M_A + M_B$. If the temporal evolution of M_A and M_B is available, then a more precise estimate of $M(A\ AND\ B)$ can be obtained.

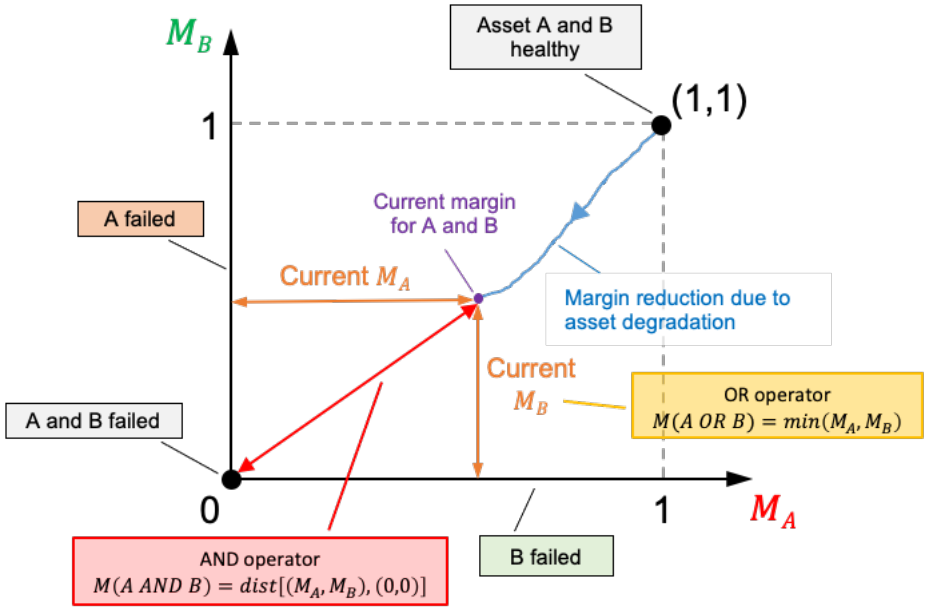

Figure 3. Graphical representation of event occurrences based on a margin framework.

Equations (1) and (2) allow us to propagate margin values through classical reliability models (e.g., fault tree or reliability block diagrams) such that we can quantify system margin. The next step is the determination of the importance (in a margin-based reliability context) of each asset. In a classical reliability setting, this is performed by relying on risk-importance measures (Lee, 2011), such as Birnbaum or Fussell-Vesely. Given the different nature of the concept of margin, we require a reliability importance measure (RIM) that captures the impact of asset margin M_α to system margin M_{sys}. Here, we rely on a classical sensitivity measure (derivative based) for an asset α defined as:

$$RIM_\alpha = \frac{\partial\, M_{sys}}{\partial\, M_\alpha} \tag{3}$$

Simply stated, RIM_α indicates how a small variation of M_α (e.g., improving the health of asset α) directly affects system margin M_{sys}.

2.1 Margin Analysis Applied to Path Sets

Reliability models (e.g., fault trees and reliability block diagrams [Lee, 2011]) can be solved symbolically by generating the MCSs of the considered system, and applying Eq.s (1) and (2) to numerically determine the margin of each MCS and the margin of the union of all the MCSs. In the context of margin-based reliability modeling, rather than considering the system MCSs, it is more suitable to rely on the concept of minimal path sets (MPSs) (Youngblood, 2001). From a reliability standpoint, these two concepts are strongly related to each other; while MCSs represent conditions under which the system can fail (failure paths), MPSs represent conditions under which the system can operate (i.e., success paths). More precisely a MCS represents a subset of assets that, when all failed, cause the system to fail. Conversely, a MPS represents a subset of assets that, when all functioning, guarantee the system to function.

Assuming the system is composed by a set of N assets; each asset i is characterized by a Boolean state variable s_i (Lee, 2011) where s_i indicates the status of such asset (*True* for a healthy asset and *False* for a failed asset). The system vector $\boldsymbol{s}$ is here defined as the ensemble of the state variables associated with all system assets: $\boldsymbol{s} = (s_1, s_2, \dots, s_N)$. It is now possible to define the system Boolean state variable $\Phi(\boldsymbol{s})$ as $\Phi(\boldsymbol{s}) = \Phi(s_1, s_2, \dots, s_N)$. From a reliability modeling perspective, $\Phi(\boldsymbol{s})$ is typically constructed by employing fault trees or reliability block diagrams. Note the $\Phi(\boldsymbol{s})$ describes – from a functional perspective – the asset dependencies at the system level. By employing Boolean logic operations, the MCSs can be obtained from $\Phi(\boldsymbol{s})$. Now, the generation of MPSs can be constructed from $\Phi(\boldsymbol{s})$ by solving $NOT[\Phi(\boldsymbol{s})]$.

The concept of margin is designed to measure the health of an asset; hence, it focuses on the operability aspect of such asset. When focusing on continuously operating systems (e.g., the secondary side of NPPs), it is relevant, from a decision-making point of view, to identify the ways that guarantee the system to operate. Hence, MPSs coupled with margin-based calculations are more suitable.

3. Integration of ER Data into Margin Models

The definition of margin presented in Section 2 is abstract; application in a more practical setting depends on the phenomena of interest and especially the available monitoring data. The scope of this section is to provide more quantitative details on how margin can be quantified depending on the available ER data.

3.1 Tech-Specs Data

As indicated in Section 2, a margin value can be calculated as the distance between actual and limiting conditions. In practical settings, limiting conditions can be represented by technical specifications of the considered asset, which are normally provided by the manufacturer. As an example, for induction motors, oil viscosity must be below a specified limiting condition to ensure proper motor function. Oil viscosity can significantly change as a function of motor rotation speed. In this context, asset margin can be calculated as the difference between the specified tech-specs limiting condition and the currently measured oil viscosity.

In general terms, given an upper limiting condition x_{LC} for a monitored variable x_{obs}, a margin M can be defined as:

$$M(x_{obs}) = \frac{x_{LC} - x_{obs}}{x_{LC} - \min(x_{obs})} \tag{4}$$

where $\min(x_{obs})$ indicates the minimum allowable value for x_{obs}. The denominator of Eq. (4) is designed to normalize the value of M in the $[0,1]$ interval. If x_{LC} is instead a lower limiting condition, then:

$$M(x_{obs}) = \frac{x_{obs} - x_{LC}}{\max(x_{obs}) - x_{LC}} \tag{5}$$

where $\max(x_{obs})$ indicates the maximum allowable value for x_{obs}.

As an example, induction motors are designed to operate within specified differential temperature limits; these limits indicate the maximum permissible difference between motor temperature and the environment temperature that various classes of insulation materials can withstand (this temperature limit can range between 80-120°C depending on the insulation material). In this scenario x_{LC} is represented by the specified temperature limit while x_{obs} is the difference between the actual motor temperature and the environment temperature.

3.2 Observed Reliability Parameters

Current industry-wide available data sets often report mean time to failure (MTTF) values for assets given past operation experience for similar assets operating in similar environmental conditions[1] (e.g., temperature and humidity). In this context, no monitoring data is available, but only past operational experience can be used. Similar to the reasoning behind Eq. (4), based on the current age t of an asset (since installation or refurbishment) and its estimated $MTTF$, margin can be defined as a linear function of t :

$$M(t) = \begin{cases} \dfrac{MTTF - t}{MTTF} & if\ t < MTTF \\ 0 & if\ t \geq MTTF \end{cases} \tag{6}$$

When the considered asset is brand new (i.e., $t = 0$), margin $M = 1$; when the same asset is approaching its estimated $MTTF$, then margin $M = 0$ (see Figure 4). Note that by this definition, margin linearly decreases as function of asset age. Similar thinking is extended to prognostic assessments where asset remaining useful life (RUL) is estimated using prognostic methods (see Section 3.5). While $MTTF$ is only based on past operational data for similar asset, RUL also accounts for health data coming from the considered asset.

[1] See https://www.nerc.com/pa/RAPA/gads/Pages/pc-GAR.aspx as an example of available reliability database.

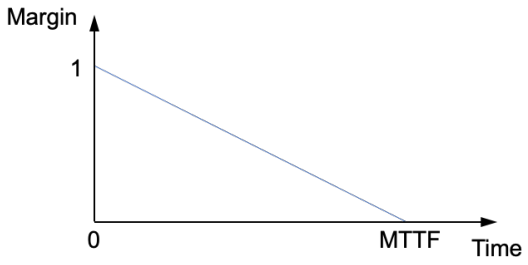

Figure 4. Graphical representation of margin when MTTF is provided.

3.3 Data Limited to Healthy Status

Here we are considering the situation were the available monitoring data for the asset under consideration has been collected exclusively when the asset was in a healthy state $\Xi^{obs-healthy}$; in other terms, data in presence of asset degradation of failure are not available. In particular, $\Xi^{obs-healthy}$ represents a collection of past observation data elements ξ^{obs}. The following notation will be used throughout the paper: a single observation data element ξ^{obs} can be composed by L observed variables x_l $(l = 1, \dots, L)$, i.e., $\xi^{obs} = [x_1, .., x_L]$; the nature of the observed variables x_l can be heterogenous in nature (e.g., temperature, pressure).

In this kind of situation, the health status of an asset can be established by measuring how actual monitoring data differ (distance wise) from healthy data. In this respect, classical statistical analysis tools designed to quantify the residual between actual observed data ξ^{obs} and predicted data ξ^{rec} (which is computed from ξ^{obs} and $\Xi^{obs-healthy}$) can be employed. Such tools can be based on kernel density estimation (e.g., auto-associative kernel regression [AAKR] method [Baraldi, 2015]) or deep-learning based methods (e.g., see [Zhang, 2019]). Under normal conditions, ξ^{rec} is very similar to ξ^{obs} (i.e., $\xi^{obs} \cong \xi^{rec}$). The condition $\xi^{obs} \neq \xi^{rec}$ indicates anomalous behavior (e.g., asset degradation).

In this context, a margin value can be then defined by measuring the difference between ξ^{rec} as ξ^{obs} as follows:

$$M(\xi^{obs}) = e^{-\left(\frac{\left\|\xi^{obs} - \xi^{rec}\right\|}{h}\right)^2} \tag{7}$$

where: $\left\|\xi^{obs} - \xi^{rec}\right\|$ indicated the residual between observed and predicted data, and h represents the comparison parameter between ξ^{rec} and ξ^{obs} (expressed in terms of standard deviation). When the asset is under normal conditions (i.e., kernel regression is located within the asset normal condition data $\Xi^{obs-healthy}$), $\xi^{obs} \cong \xi^{rec}$; hence $M = 1$. If the asset is under abnormal conditions, the norm of the difference between ξ^{obs} and ξ^{rec}increases, and consequently M drops to 0.

Note that it is here assumed that $\Xi^{obs-healthy}$ covers all possible healthy conditions of the asset. If this is not the case, then when ξ^{obs} reaches unobserved healthy conditions, the obtained margin value will reflect the fact that the asset is not healthy. However, once newly observed healthy conditions are recorded, they can be added to the original data set $\Xi^{obs-healthy}$.

An example is shown in Figure 5, where a set $\Xi^{obs-healthy}$ of observed data elements $\xi^{obs} = [x_1, x_2]$ is collected (green dots in Figure 5-left). Actual observed data ξ^{obs} are constantly recorded while ξ^{rec} are determined based on ξ^{obs} and $\Xi^{obs-healthy}$ (see black and red lines in Figure 5-left) using the AAKR method (Baraldi, 2015). By applying Eq. (7) to this test case it is possible to generate a temporal profile for the corresponding margin (see Figure 5-right).

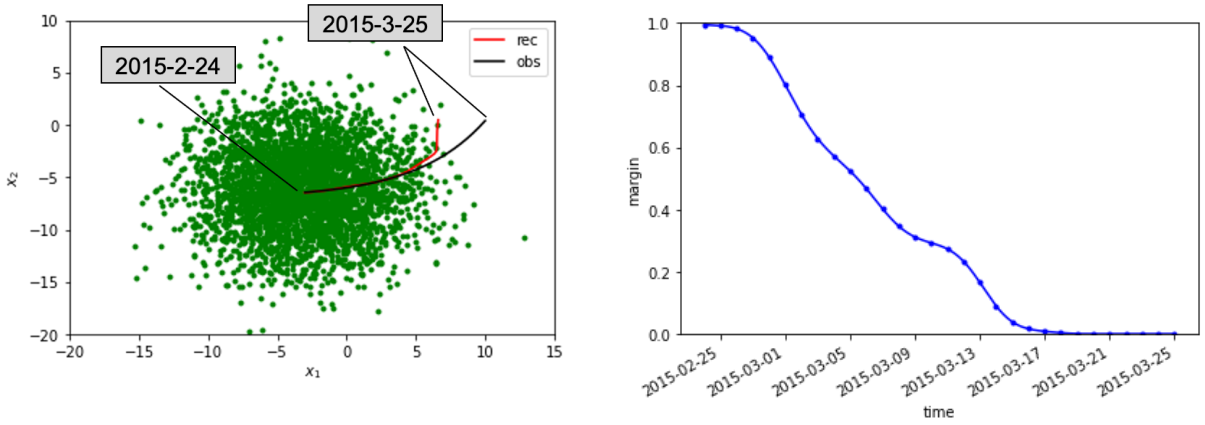

Figure 5. Representation of $\Xi^{obs-healthy}$ (green population), ξ^{obs} (black line), and ξ^{rec} (red line) in the x_1, x_2 space (left figure); temporal profile of the corresponding margin (right figure).

3.4 Condition Based Data

This situation extends the one described in Section 3.3, where data under healthy conditions $\Xi^{obs-healthy}$ are available, by incorporating data under faulty conditions, indicated here as $\Xi^{obs-faulty}$. It is assumed that in the presence of an asset fault, actual observed data ξ^{obs} can be seen transitioning from $\Xi^{obs-healthy}$ toward $\Xi^{obs-faulty}$.

In this scenario, by following the definition of margin presented in Section 2, and provided actual observed data ξ^{obs} (along with historic healthy $\Xi^{obs-healthy}$ and failed data $\Xi^{obs-faulty}$), a margin value can be determined by comparing the mutual distance of ξ^{obs} from the two populations, $\Xi^{obs-healthy}$ and $\Xi^{obs-faulty}$ (see Figure 6). In mathematical form, a margin can be written as:

$$M\left(\xi^{obs}\right) = \frac{D\left(\xi^{obs}; \Xi^{obs-faulty}\right)}{D\left(\xi^{obs}; \Xi^{obs-faulty}\right) + D\left(\xi^{obs}; \Xi^{obs-healthy}\right)} \tag{8}$$

where the operator $D(.;.)$ represents the distance one single data element (i.e., ξ^{obs}) and a population of data elements (either $\Xi^{obs-healthy}$ or $\Xi^{obs-faulty}$). The choice of the operator $D(.;.)$ might depend on several factors dictated by the distribution of the $\Xi^{obs-healthy}$ and $\Xi^{obs-faulty}$ population in the data space. Selected options of the operator $D(.;.)$ using classical statistical analysis considerations are indicated below:

$$D\left(\xi^{obs}; \Xi\right) = \min\left\{d\left(\xi^{obs}, \xi\right): \xi \in \Xi\right\} \tag{9}$$

$$D\left(\xi^{obs}; \Xi\right) = \text{avg}\left\{d\left(\xi^{obs}, \xi\right): \xi \in \Xi\right\} \tag{10}$$

$$D\left(\xi^{obs}; \Xi\right) = p_{5\%}\left\{d\left(\xi^{obs}, \xi\right): \xi \in \Xi\right\} \tag{11}$$

where $d\left(\xi^{obs}, \xi\right)$ indicates the Euclidean distance between two observations (i.e., ξ^{obs}, ξ), and $p_{5\%}^{RUL}$ indicates the 5th percentile of the considered population.

These three options rely on determining the distance between ξ^{obs} and all the elements contained in Ξ; the first one considers the smallest distance value (i.e., the point in Ξ that is the closest to ξ^{obs}) while the second one averages all distance values.

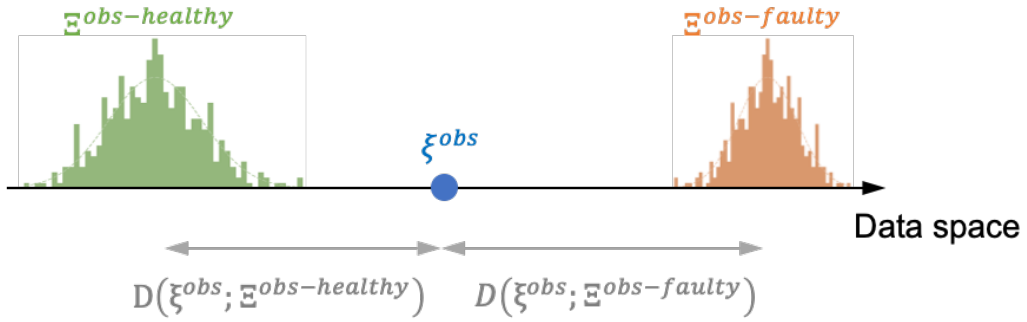

Figure 6. Margin calculation given current asset monitoring status ξ^{obs} when both healthy $\Xi^{obs-healthy}$ and faulty $\Xi^{obs-faulty}$ data are available in the $[x_1, .., x_L]$ data space.

Note that a distance-based approach for $D(\xi^{obs}; \Xi)$ works well when healthy and faulty data are well separated in the $[x_1, .., x_L]$ space. In practical scenarios, the two populations of data elements (i.e., faulty and healthy) might overlap. In this case, margin can be quantified using density-based methods (Hastie, Tibshirani, and Friedman 2001); these methods are designed to translate (e.g., through kernel density estimation methods) the $\Xi^{obs-healthy}$ and $\Xi^{obs-faulty}$ datasets into probability distribution functions (pdfs): $pdf^{healthy}$ and pdf^{faulty}. Then, given a current observed measurement ξ^{obs}, margin can be quantified by evaluating these two pdfs at the coordinate ξ^{obs} as follows:

$$M(\xi^{obs}) = \frac{pdf^{healthy}(\xi^{obs})}{pdf^{healthy}(\xi^{obs}) + pdf^{faulty}(\xi^{obs})} \tag{12}$$

This equation weights the pdf values at coordinate ξ^{obs} for both healthy and faulty conditions; when ξ^{obs} is located in a region of the $[x_1, .., x_L]$ space dominated by healthy data, then $pdf^{healthy}(\xi^{obs}) \gg pdf^{faulty}(\xi^{obs})$, and $M(\xi^{obs}) \cong 1.0$. Conversely, when ξ^{obs} is located in a region of the $[x_1, .., x_L]$ space dominated by faulty data, then $pdf^{healthy}(\xi^{obs}) \ll pdf^{faulty}(\xi^{obs})$, and $M(\xi^{obs}) \cong 0.0$.

An example that extends the one shown in Section 3.3 is now considered where $\Xi^{obs-healthy}$, and $\Xi^{obs-faulty}$ are shown in the left plot of Figure 7, ξ^{obs} is here represented as the black line moving from left to right; the corresponding margin is shown in the right plot of Figure 7. Here, $pdf^{healthy}(\xi^{obs})$ and $pdf^{faulty}(\xi^{obs})$ were generated using kernel density estimation methods (Hastie, Tibshirani, and Friedman 2001).

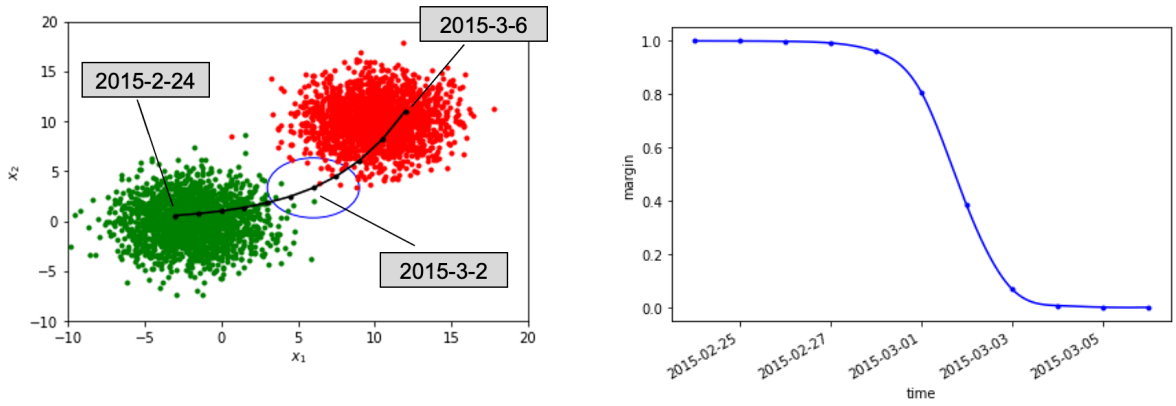

Figure 7. Representation of $\Xi^{obs-healthy}$ (green population), $\Xi^{obs-faulty}$ (red population), and ξ^{obs} (black line), in the x_1, x_2 space (left figure); temporal profile of the corresponding margin (right figure).

An alternative formulation to Eq. (12) can be derived when machine learning (ML) methods (Mohri, 2012) are employed. In this setting, a supervised ML model (i.e., a classifier) is trained using both faulty and healthy datasets ($\Xi^{obs-faulty}$, $\Xi^{obs-healthy}$), and it is employed to predict, given ξ^{obs}, the class out (either faulty or healthy) that ξ^{obs} belongs to. Such prediction can be augmented by also determining the probability estimate $Prob^{detec}$ associated with the prediction out. If the [0,1] margin interval is divided into two equally long segments, then we can assign the class "healthy" to the [.5,1] interval and the class "faulty" to the $[0, .5]$ interval. Hence, the predicted class out generated by the ML model determines the margin variability interval (either $[0, .5]$ or [.5,1]). The variable $Prob^{detec}$ is essentially a measure of how accurate the prediction is. More precisely, a high value of $Prob^{detec}$ implies high accuracy in the prediction; conversely, a very low value implies low accuracy. In this context, $Prob^{detec}$ is here used to determine the precise margin location in the $[0, .5]$ or [.5,1] intervals. A high value of $Prob^{detec}$ would drive margin toward the extreme of the intervals (either 0 or 1); a low value of $Prob^{detec}$ would drive margin toward the common point of the intervals (i.e., 0.5).

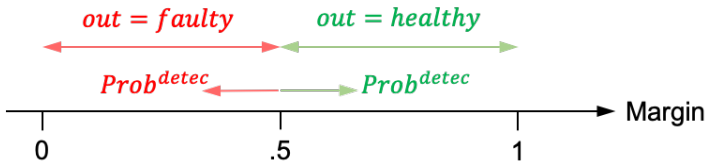

Figure 8. Graphical representation of margin provided out and $Prob^{detec}$ of a ML model.

Consequently, provided ξ^{obs} and a ML model which can generate both out and $Prob^{detec}$, a margin value can be defined as follows:

$$M(\xi^{obs}) = \begin{cases} 0.5 - \dfrac{Prob^{detec}}{2} & if\ out = faulty \\ 0.5 + \dfrac{Prob^{detec}}{2} & if\ out = healthy \end{cases} \quad (13)$$

Deep neural network (Hastie, Tibshirani, and Friedman, 2001) based models are a class of ML models widely employed for diagnostic applications. This class of classifier models, given ξ^{obs}, generates the class

out (either faulty or healthy) that ξ^{obs} belongs to, and a probability value associated with each class: $Prob^{healthy}$ and $Prob^{faulty}$ (rather than a single probability value $Prob^{detec}$). Note that if two classes are considered (faulty and healthy), then $Prob^{healthy} + Prob^{faulty} = 1$. The variable out is determined as follows:

$$out = \begin{cases} healthy & if\ Prob^{healthy} > Prob^{faulty} \\ faulty & if\ Prob^{healthy} < Prob^{faulty} \end{cases} \quad (14)$$

In this context, margin quantification employs directly the two generated probability values (i.e., $Prob^{healthy}$ and $Prob^{faulty}$) as follows:

$$M\left(\xi^{obs}\right) = Prob^{healthy} = 1 - Prob^{faulty} \quad (15)$$

3.5 Prognostic Data

Estimation of the RUL of an asset provides valuable information about its failure time. Given the stochastic nature of the failure phenomena, RUL is typically expressed in terms of a probabilistic distribution along the temporal axis. A large number of methods have been developed in the literature to predict RUL for specific assets, and (Ferreira and Gonçalves, 2022) provides a summary of the most widely used methods. For the goal of integrating the RUL pdf (indicated here as PDF_{RUL}) into a margin-based reliability model, similar reasoning presented in Section 3.2 is here applied. A margin is defined as the distance between actual time and the predicted RUL. The main differences are that: 1) RUL is estimated once a degradation mechanism is identified (e.g., through an anomaly detection method as indicated in Section 3.3), and 2) RUL is an actual distribution function rather than a point value (as indicated in Section 3.2).

Once the RUL pdf is estimated, determination of the corresponding margin value can be estimated using two approaches. The first defines the margin as:

$$M(t) = 1 - CDF_{RUL}(t) \quad (16)$$

where CDF_{RUL} indicates the cumulative distribution function corresponding to PDF_{RUL}. The second approach estimates margin as the distance between the actual asset life and a point estimate of the RUL distribution (e.g., the 5th percentile $p_{5\%}^{RUL}$) as follows:

$$M(t) = \frac{p_{5\%}^{RUL} - t}{p_{5\%}^{RUL}} \quad (17)$$

where $p_{5\%}^{RUL}$ indicates the 5th percentile of the RUL distribution PDF_{RUL}.

A graphical representation of the margins for both approaches is shown in Figure 9 for an estimated RUL normally distributed as shown in red. Note that the proposed approach updates the margin value when asset health is measured and when a better RUL estimation (i.e., less uncertainty associated with RUL) is available from the corresponding prognostic model.

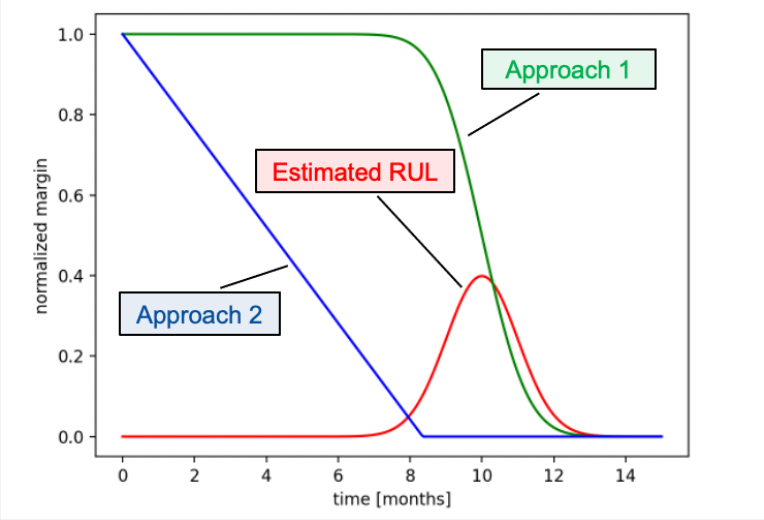

Figure 9. Margin values obtained from the two proposed approaches (green and blue lines) given an estimate of asset's RUL (red line).

Before initial degradation is detected (meaning RUL cannot be estimated yet), asset margin is set to 1.0 (asset healthy). Once asset degradation is observed and RUL pdf estimation is available, the corresponding margin value is then updated using the same estimators indicated in Eqs. (16) or (17).

3.6 Example 1: Single asset with multiple failure modes

In most practical settings, multiple failure modes might be present for a single asset, and the installed monitoring system is designed to detect a subset of these failure modes. In this case, asset failure can be induced by any of the considered failure modes. Figure 10 provides an example where an asset has four identified failure modes and three monitoring systems that can identify one (or more) failure modes. In more detail, each monitoring system can generate one or more observed variables x_l, and the estimation of the margin associated with each failure mode might require observed variables generated by multiple monitoring systems.

Using the analysis methods provided in Sections 3.1 through 3.4, a margin value for each failure mode (M_1, M_2, M_3, M_4) can be determined where:

$$\begin{aligned} M_1 &= M_1(x_1, x_2) \\ M_2 &= M_2(x_1, x_2, x_3, x_4, x_5) \\ M_3 &= M_3(x_3, x_4, x_5) \\ M_4 &= M_4(x_6) \end{aligned} \tag{18}$$

Assuming the failure of the considered asset can occur from any of the four failure modes, then (see Section 2) it is possible to determine margin associated with the considered asset:

$$M = \min(M_1, M_2, M_3, M_4). \tag{19}$$

Note that this is an intuitive interpretation of asset health since, in this case, it is driven by the failure mode with lowest margin.

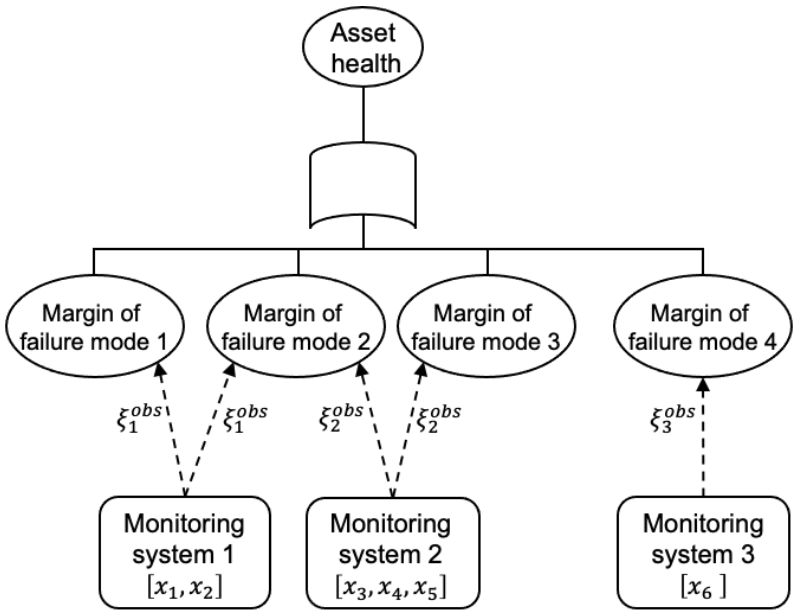

Figure 10. Decomposition of asset health as equal contribution all failure modes.

3.7 Example 2: Multi-Asset System

A margin-based reliability calculation example is indicated here for the system shown in Figure 11 (Youngblood 2001) composed of seven assets, labeled A through G. For each asset, an estimation of its margin is provided (see Figure 12). Margin estimation for assets A and E have been generated by their estimated RUL. The RUL estimation is represented here probabilistically, that is, the RUL is represented by a pdf designed to represent the uncertainty associated with a RUL estimate. For assets B, C, and D, margins were estimated from online monitoring data that is continuously available. Margins for assets F and G were estimated from data available at discrete instances (e.g., through manual testing/surveillance operation). In this example, we let the assets degrade until they are considered inoperable (i.e., we do not allow maintenance operations to restore their health); this setting is designed to track the temporal profile of asset margin, and to illustrate how asset margin values affect system margin through their RIM measure.

As indicated in Section 2.1, we represent system reliability in terms of MPSs rather than MCSs. The obtained list of MPSs is as follows:

$$MPS = [A, BCD, BEG, BFG]. \tag{20}$$

The temporal profile of system margin was calculated, for each time step, by considering the MPSs listed above, the margin value of all assets, and applying the rules indicated in Section 2.

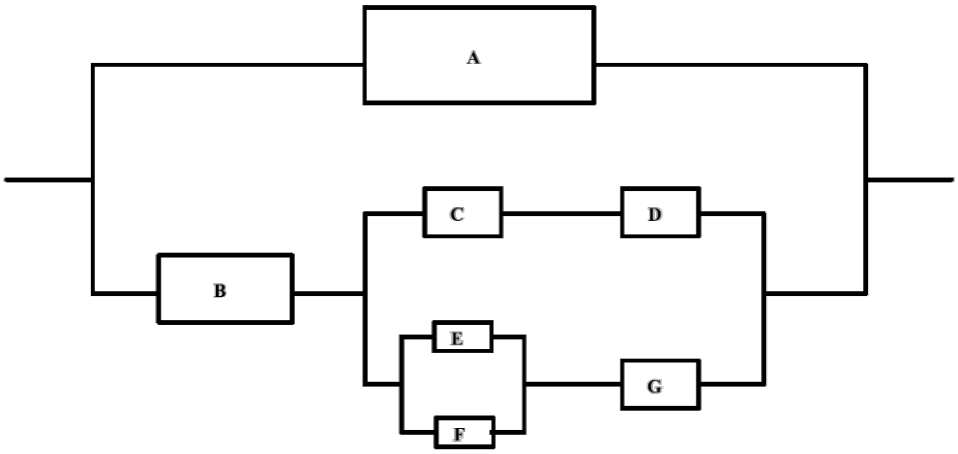

Figure 11. Example of system architecture represented in terms of block diagrams (Youngblood 2001).

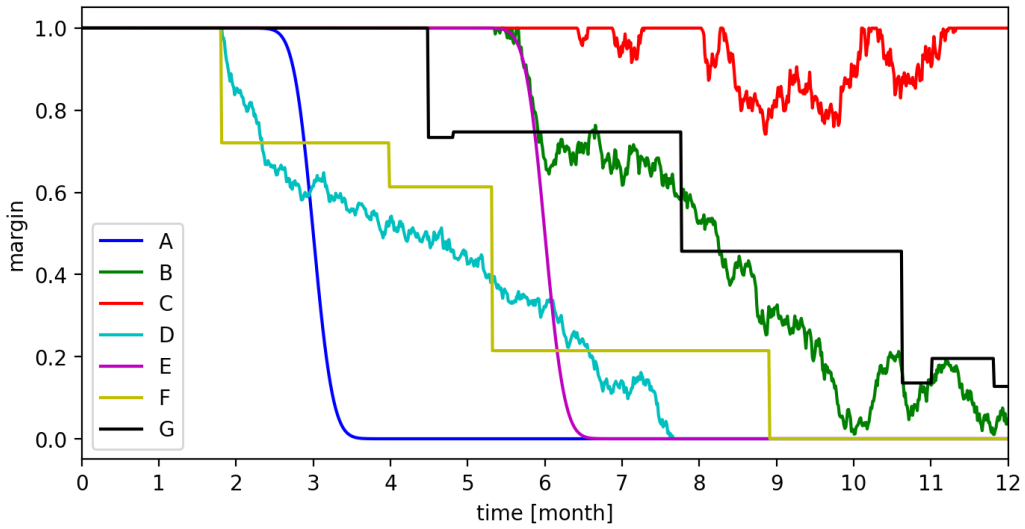

Figure 12. Temporal profile of the margin associated with each asset of the system indicated in Figure 11.

The obtained temporal profile of system margin is shown in Figure 13. From this plot, note the following:

1. Even though asset margin is defined in the [0,1] interval, system margin can be higher than one (but still cannot be negative). A system margin greater than one implies that there are redundancies that can compensate for asset unavailability (e.g., due to failure or maintenance operations). In other terms, when there is more than one single MPS, the system margin is greater than one. At time $t = 0$, there are four MPSs, and the margin for each asset is set to one, hence the system margin can be calculated as $\sqrt{1+1+1+1} = 2.0$.
2. Due to asset degradation, asset margin decreases until it reaches 0. Once this happens, a MPS might become unavailable. As an example, at time t= 3 $months$, asset A fails and, hence, the number of available MPSs decrease from four to three.

3. For assets A and E, Eq. (16) was used to determine margin values provided their RUL distribution.
4. At time $t = 8.9\ months$, asset F fails, and even though assets C, B and G are working properly, there are no available MPSs and, consequently, the system margin value drops to zero.

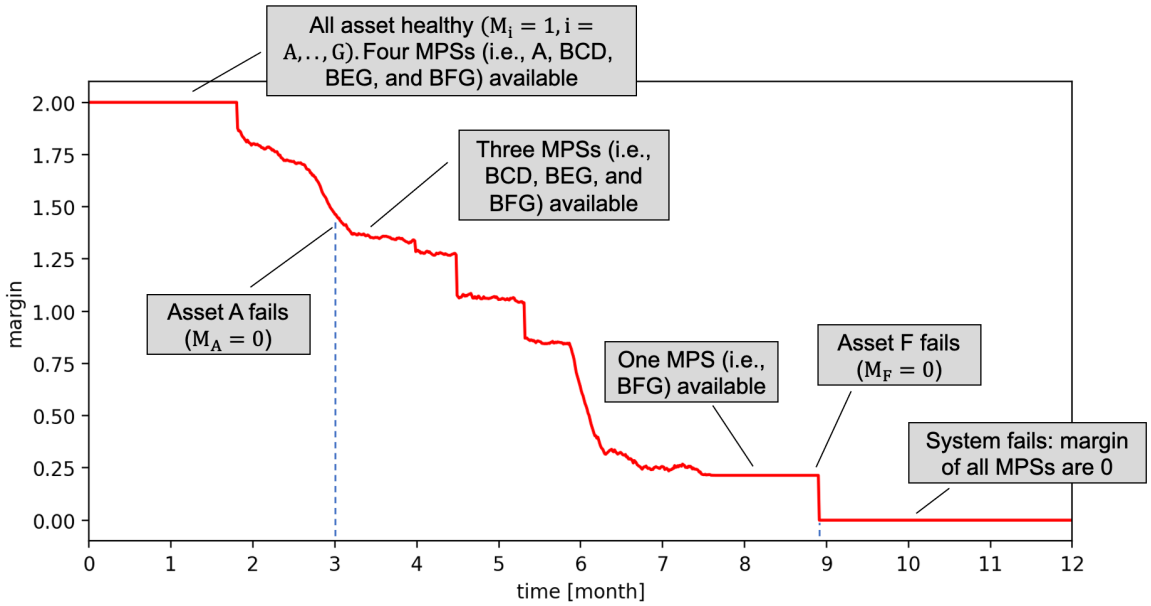

Figure 13. Temporal profile of system margin provided the asset margin indicated in Figure 12.

The next step is quantification of the RIM measures indicated in Section 2 (see Eq. [3]). For each asset, these measures were calculated based on the system margin at each time instant (see Figure 12 and Figure 13). Figure 14 presents the temporal profile of the RIM measure for all assets along with the temporal profile of each MPS (top plot of Figure 14). The key information elements to be considered in the RIM analysis are basically two: 1) the number of MPSs that an asset is supporting, and 2) the margin value of an asset compared to the margin value of the other assets that are part of the same MPS.

In order to show the type of information generated by these plots, note the following:

1. $t = 0\ months$: all assets are healthy but RIM values for the considered assets are not identical; in fact, a higher RIM value is indication that the same asset is supporting multiple MPSs. In this particular situation, asset B has highest RIM value since it supports 3 out of 4 MPSs.
2. $t = 2\ months$: all assets are still healthy, but assets F and D are showing degradation signs. This impacts the health value of two MPSs (BCD and BFG). The importance of asset B is now dropping since the health of these two MPSs is driven by F and D.
3. $t = 3.5\ months$: asset A fails and three MPSs are now available (BCD, BEG, BFG). Obviously, importance of asset A decreases.
4. $t = 4.5\ months$: three MPSs are still available (BCD, BEG, BFG) while assets G, F, and D now have margin values less than 1. In this scenario, importance of B and E drop since now assets G, F and D are driving system margin.
5. $t = 5.8\ months$: three MPSs are still available (BCD, BEG, BFG), where $M_C = 1$ and $M_B > M_G > M_E > M_D > M_F$. Hence, importance is higher for assets D, E and F since they are driving margin of the three remaining MPSs.
6. $t = 8.5\ months$: only one MPS is still available (BFG), and $M_C > M_G > M_B > M_F$. Again, importance is driven by the asset with lowest margin value (i.e., F).

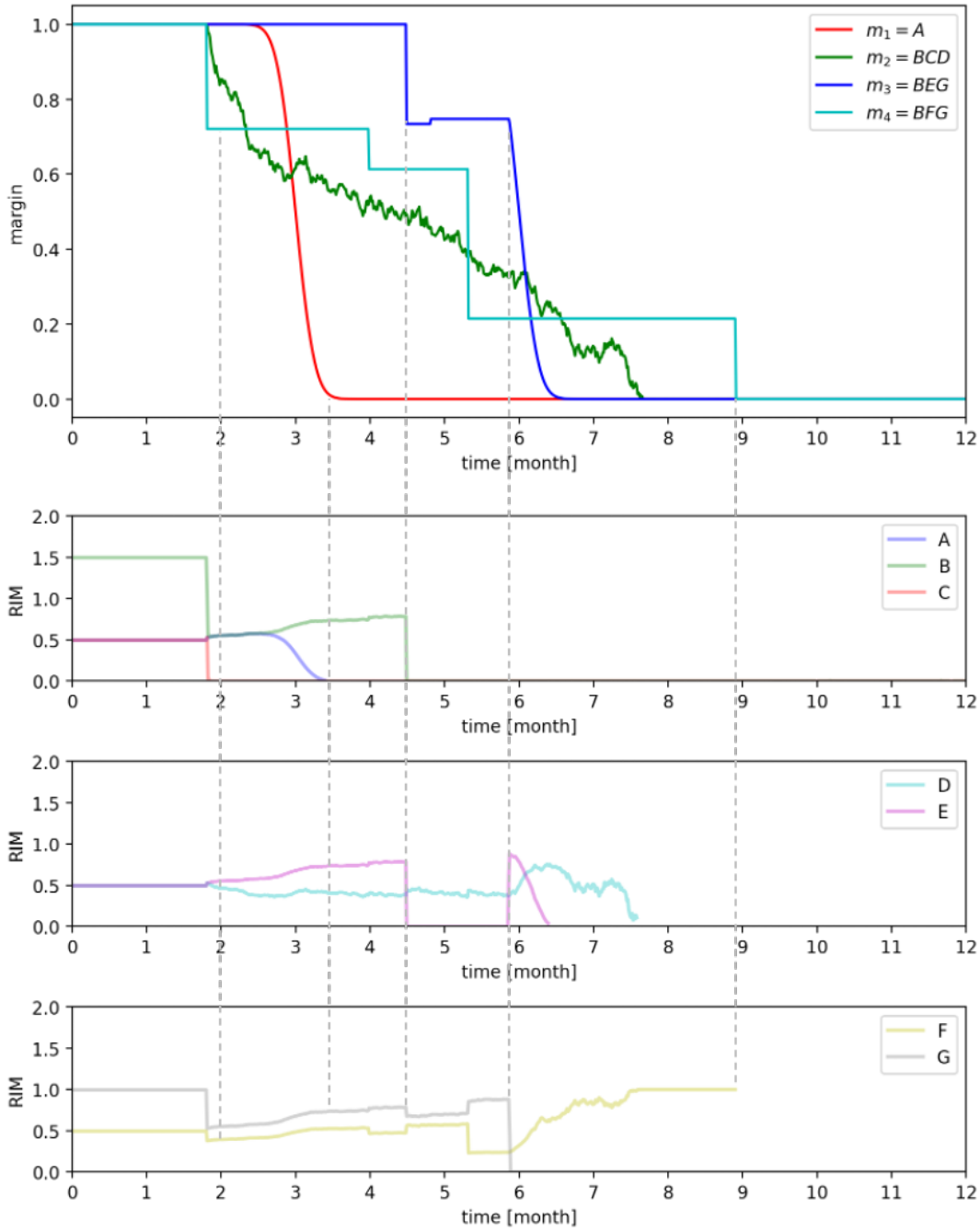

Figure 14. Plot of RIM measures for the seven assets of the system of Figure 11 given the provided margin data.

3.8 Comparison of Classical and Margin-Based Reliability Modeling

Reference (Mandelli, 2022) provides an initial comparison of classical and margin-based reliability modeling. These differences can be described though a cause-effect lens. Classical reliability models focus on the *effect node* where asset reliability data are used to assess the system failure probability. Such models

monitor plant risk (as currently done by plant risk monitors), and are used to support "static" decisions such as determining the frequency of periodic surveillance and maintenance activities, or setting the duration of planned system maintenance outages (either as part of a plant configuration risk-management program or a plant risk-managed technical specification program).

Over the past several decades, plants have been moving from a reliance on periodic preventive maintenance to more comprehensive predictive maintenance strategies where the goal is to only perform intrusive maintenance operations when needed. Advanced monitoring and data analysis technologies are essential to support predictive strategies. This is where margin-based reliability approaches can support "dynamic" decision-making where, based on current monitoring data, asset health data are employed to assess asset and system health, i.e., the focus is now shifted to the *cause node*.

The goal of this section is to provide a more concrete bridge between margin and classical reliability approaches, complementing the initial comparison of classical and margin-based reliability modeling presented in (Mandelli, 2022). A common ground for these two kinds of reliability approaches can be established if available ER data is composed solely of asset MTTF values. In this scenario, we are considering the failure time value for each asset; the objective is to determine system failure time for the most common system configurations: series, parallel, stand-by, and K out of N (KooN).

Given the failure rate for the considered assets, the corresponding MTTF values can be calculated. Using the set of equations provided by (Rausan, 2020) – which are summarized in Table 1 – it is possible to determine system failure time of the considered system configurations based on classical reliability theory. System failure time can be calculated from the failure time of two assets (i.e., T_1, T_2) for the considered configurations (see central column of Table 2).

Table 1. Summary of reliability and MTTF equations for several configurations (Rausand, 2020).

Configuration	Reliability	MTTF
Series	$\prod_{i=1}^{N} R_i(t)$	$\frac{1}{\sum_{i=1}^{N}\lambda}$
Parallel	$1-\prod_{i=1}^{N}\left(1-R_i(t)\right)$	$\frac{1}{\lambda}\sum_{i=1}^{N}\binom{N}{i}\frac{(-1)^{i+1}}{i}$
Stand-by	$R_1(t)+\lambda\, t\, R_2(t)$	$\frac{1}{\lambda}+\frac{1}{\lambda}=\frac{2}{\lambda}$
KooN	$\sum_{i=k}^{N}\binom{N}{i}R(t)^i(1-R(t))^{N-i}$	$M\sum_{i=k}^{N}\binom{N}{i}\int_0^{\infty}R(t)^i(1-R(t))^{N-i}$

Similarly, asset MTTF values can be translated in terms of margins with the goal of determining system margin for the considered system configurations using the equations provided in Section 2. In this situation, a margin is basically the distance between actual asset life and its predicted failure time (i.e., the asset MTTF). The system margin M_{sys} values for the considered system configurations are presented in the right column of Table 2.

The goal now is to translate M_{sys} values back into time values to compare with T_{sys}. We expect that this comparison process will provide identical outcomes from classical and margin reliability methods. At a first look at Table 2, the mathematical expressions for T_{sys} and M_{sys} for the series, stand-by, and KooN configurations are very similar. Recall that assets margin values are defined over the time axis and quantified based on asset MTTF; hence, the translation from M_{sys} to system failure time in a margin-based reliability context gives these outcomes:

- *Series*: given that M_{sys} is defined over a minimum of two asset margins, the system failure time derived from margin calculation corresponds to $min(T_1, T_2)$ (see Figure 15).
- *Parallel*: in this configuration, M_{sys} follows the path shown in Figure 16 where assets fail at two different time instances while system fails when the latter failure occurs (i.e., $max(T_1, T_2)$).
- *Stand-by*: in this configuration, the sum of two margin values (i.e., $M_1 + M_2$) is translated into the sum of failure time of both assets (i.e., $T_1 + T_2$). Note that, in this configuration, $M_{sys} = M(A\ AND\ B)$; if the Manhattan distance is used, $M_{sys} = M_1 + M_2$ (see Figure 17).
- *KooN*: similar to the series configurations, only K assets with highest margin values are considered (and consequently the highest failure times). The minimum out of these K values gives the same outcome as min(first K highest T_i).

In conclusion, note how the above time considerations from M_{sys} (right column of Table 2) match the formulation of T_{sys} for the four considered configurations (central column of Table 2). Hence, classical and margin reliability approaches converge within the same context, i.e., when dealing with MTTF values. However, classical reliability modeling fails when dealing with sensor data, anomaly detection, or diagnostic or prognostic modeling results.

Table 2. Comparison between system failure time and system margin for four system configurations.

Configuration	**System failure time T_{sys}**	**System margin M_{sys}**
Series	$min(T_1, T_2)$	$min(M_1, M_2)$
Parallel	$max(T_1, T_2)$	$dist[(0,0), (M_1, M_2)]$
Stand-by	$T_1 + T_2$	$M_1 + M_2$
KooN	min(first K highest T_i)	min(first K highest M_i)

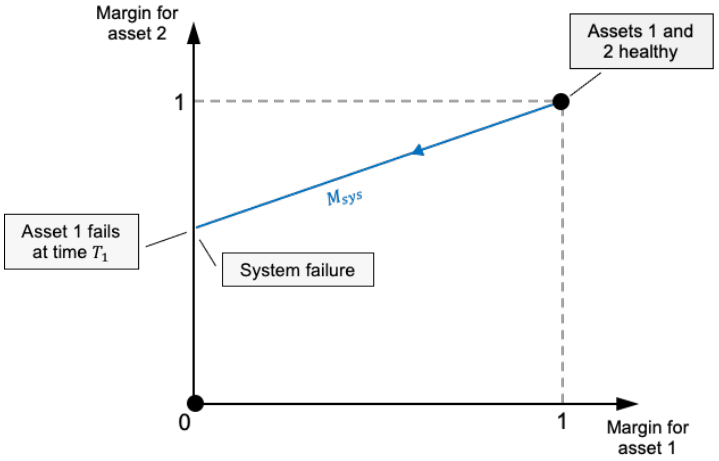

Figure 15. Evolution of M_{sys} for two assets in a series configuration.

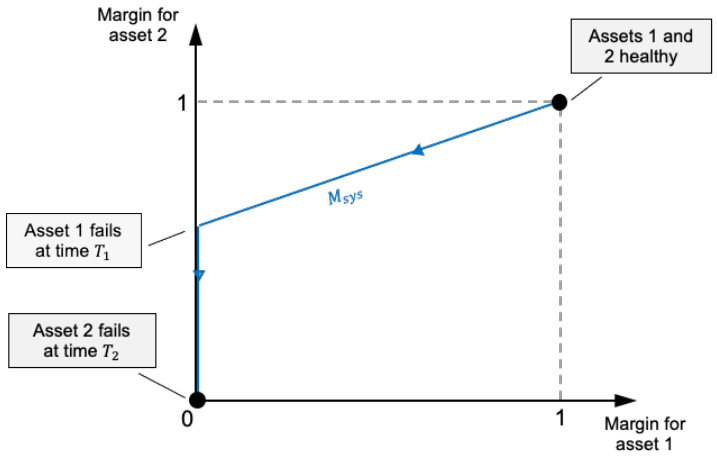

Figure 16. Evolution of M_{sys} for two assets in a parallel configuration.

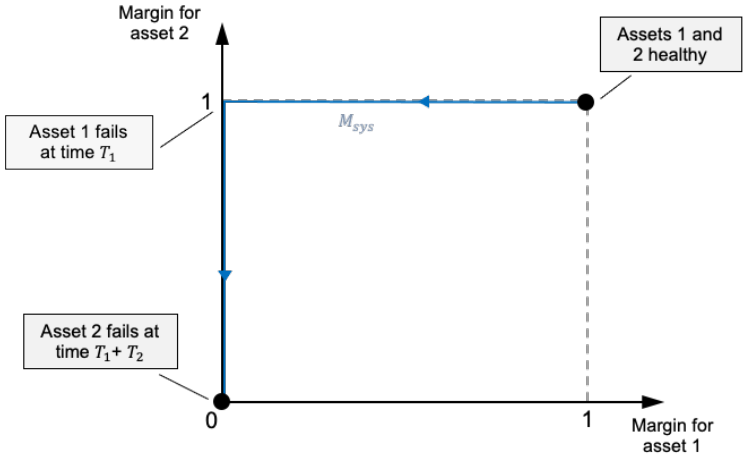

Figure 17. Evolution of M_{sys} for two assets in a stand-by configuration.

4. Test Case: CWS System

4.1 System Description and Available Monitoring Data

To develop initial methods and models, the CWS at a Public Service Enterprise Group (PSEG) Nuclear, LLC (PSEG)-owned plant site was selected as the target plant asset. The CWS is an important non-safety-related system. As the heat sink for the main steam turbine and associated auxiliaries, the CWS is designed to maximize steam power cycle efficiency (Agarwal, V. et al. 2021a, Agarwal, V. et al. 2021b). A CWS consists of the following major equipment (Agarwal, V. et al. 2021a, Agarwal, V. et al. 2021b):

- Vertical, motor-driven circulating pumps (i.e., “circulators”), each with an associated fixed trash rack and traveling screen at the pump intake to filter out debris and marine life
- Main condenser
- Condenser waterbox air removal system
- Circulating water sampling system

- Screen wash system
- Necessary piping, valves, and instrumentation/controls to support system operation.

The selected plant site (a two-unit pressurized water reactor) features six circulators at each unit. Schematic representations of the main condensers for Plant Site Unit 2 are shown in Figure 18. Each pair of waterboxes is named using the following convention: Unit #, Condenser #A, and Unit #, Condenser #B.

In this research, the project team focused on optimizing the maintenance strategy for the CWS. To differentiate between motor and pump maintenance activities for each circulator, those assets are hereafter referred to as the CWP motor and the CWP. Figure 19 shows different locations on the CWP motor where measurements are continuously collected as part of the plant OSI PI historian.

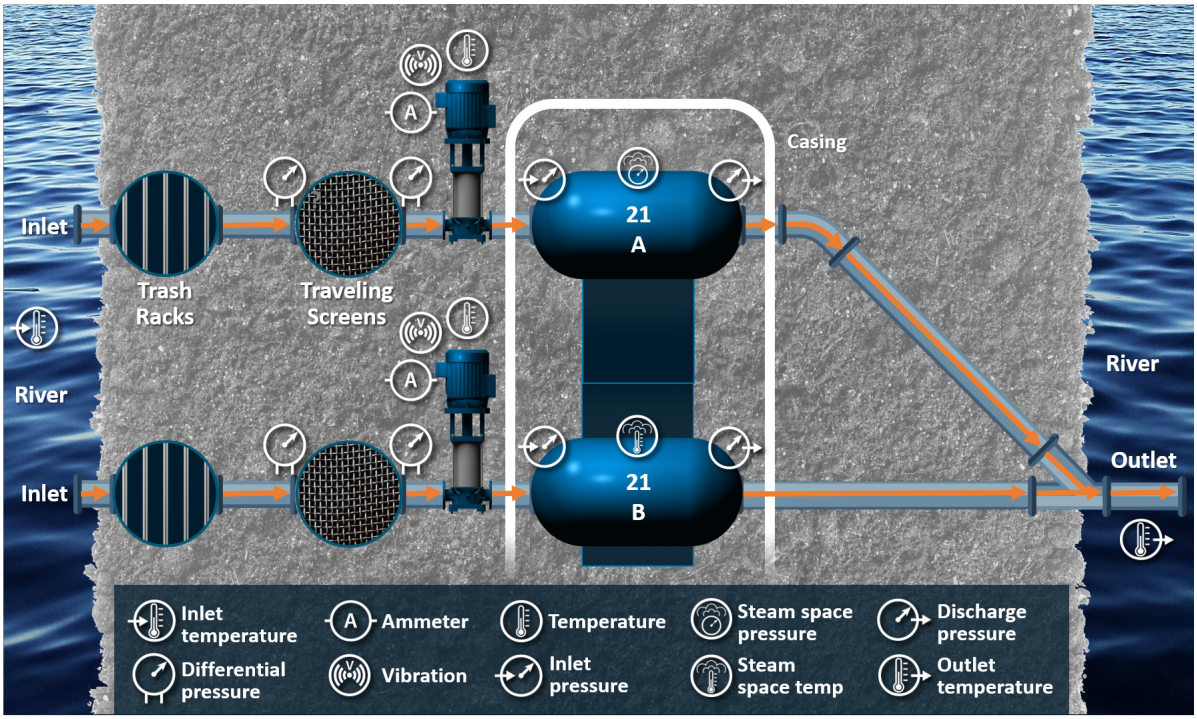

Figure 18. Plant Site Unit 2 CWP combination of 21A and 21B with sensors and instrumentation.

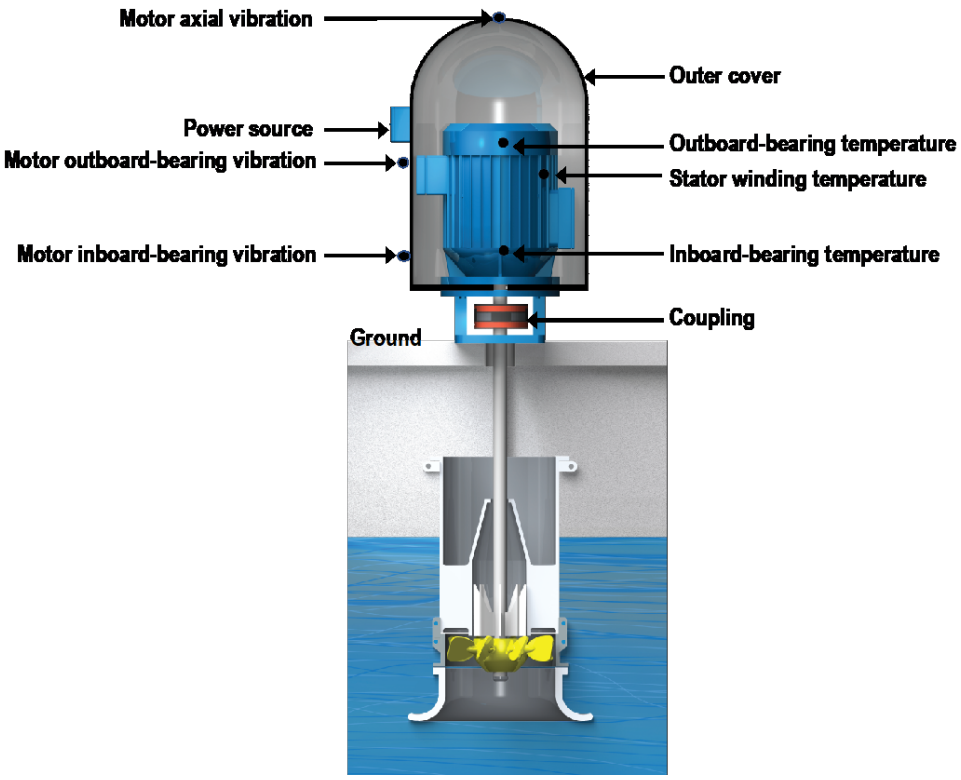

Figure 19. Schematic representation of a CWS motor and pump, along with measurement locations.

The Unit 1 and Unit 2 CWS process data are collected once every minute and stored in the Plant Site 1 OSI PI system. Due to file size restrictions, the project team received CWS process data on an hourly frequency for both units, from 2009 to 2019. The process data includes:

- Gross load (MWe)
- River level (ft)
- Ambient air temperature (°F)
- CWP inlet river temperature (°F)
- CWP outlet water temperature (°F)
- CWP motor status (ON or OFF)
- CWP motor stator winding temperature (°F)
- CWP motor inboard-bearing (MIB) temperature (°F)
- CWP motor outboard-bearing (MOB) temperature (°F)
- CWP motor current (amps)

4.2 Data Processing

As indicated in (Agarwal, V. et al. 2021a.), the raw data collected from the NPP is distributed over several data sources, and it has been processed by completing the following steps:

1. Text data is converted into numeric form (e.g., ON/OFF data element is converted into 0/1)

2. New features are generated (e.g., pump differential temperature [DT], pump age since refurbishment)
3. Pump vibration data is processed through a fast Fourier transform algorithm and magnitude of the vibration signal for specific frequencies[2] are captured
4. Based on system operational history (e.g., maintenance records), data elements are labeled (either healthy or faulty states)
5. Resolve missing data entries
6. Resolution of data conflicts between operational history and recorded numerical value
7. Merge all data sources into a single time series
8. Z-normalize all features of the time (each feature x is transformed into $\tilde{x} = \frac{x - mean(x)}{std\_dev(x)}$ where the operators $mean(x)$ and $std\_dev(x)$ correspond to mean value and the stand deviation of the considered variable x.

A series of plots of the pre-processed time series is shown in Figure 20.

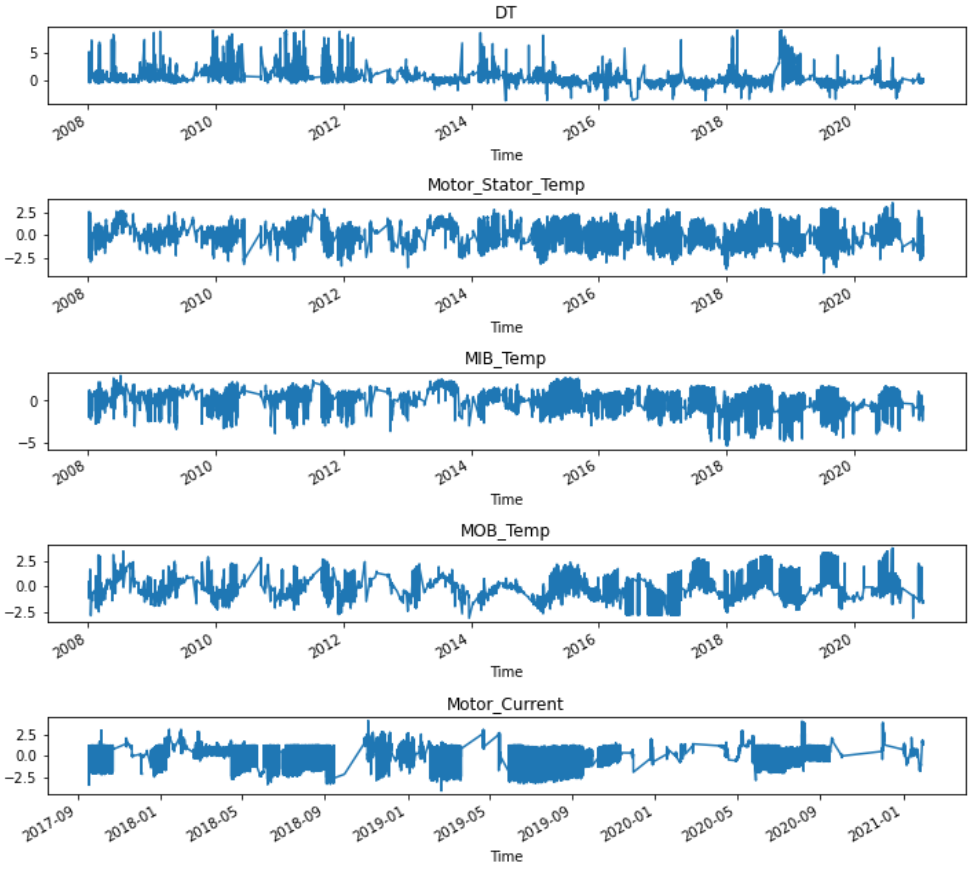

Figure 20. Plot of five features of the pre-processed time series. Note that online motor current data is available from 2017, while process variables are available from 2009.

[2] Motor running speed is set to 294 rpm (i.e., 4.9Hz). Considered motor has 4 vanes while diffuser has 6 stationary vanes. Given this layout, the considered frequencies are:

- 4.9 Hz: Fundamental harmonic
- 4.9 $Hz \cdot 4 = 19.6\ Hz$: Harmonic caused by the pump vanes
- 4.9 $Hz \cdot 6 = 29.4\ Hz$: Harmonic caused by the diffuser vanes
- 4.9 $Hz \cdot 4 \cdot 6 = 117.6\ Hz$: Harmonic caused by the combination of the pump and diffuser vanes
- 120 Hz: Vibration caused by the electric line frequency

Once the time series has been obtained, we investigated how healthy and faulty states change feature distribution. In this respect, Figure 21 shows the box plot of four considered features for the considered healthy and faulty states. These variables were chosen based on their coverage of all healthy and faulty states. Note that the structure of box plots shifts between healthy and faulty states. This is essential to correctly capture system health from available monitoring data. Note that the box plots of Figure 21 perform a comparison between healthy and faulty states by looking at the distribution of a single feature at a time. In order to capture the correlations among features for healthy and faulty states it is possible to look at feature distribution using parallel coordinate plots (see Figure 22 and Figure 23).

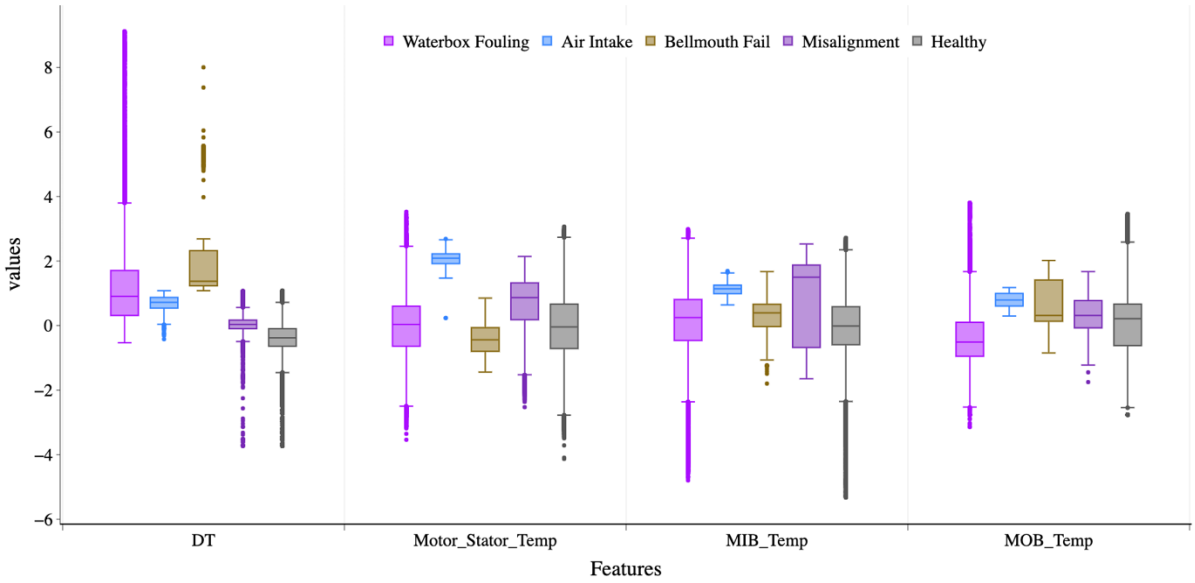

Figure 21. Box plots of four of the considered features (DT, motor stator temperature, MIB, and MOB temperatures) for healthy and failure states.

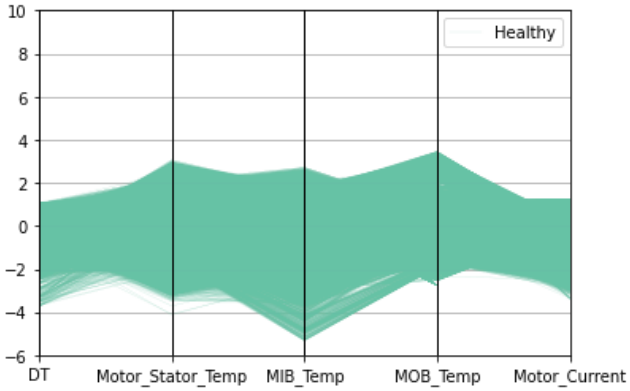

Figure 22. Parallel coordinate plots for the healthy state.

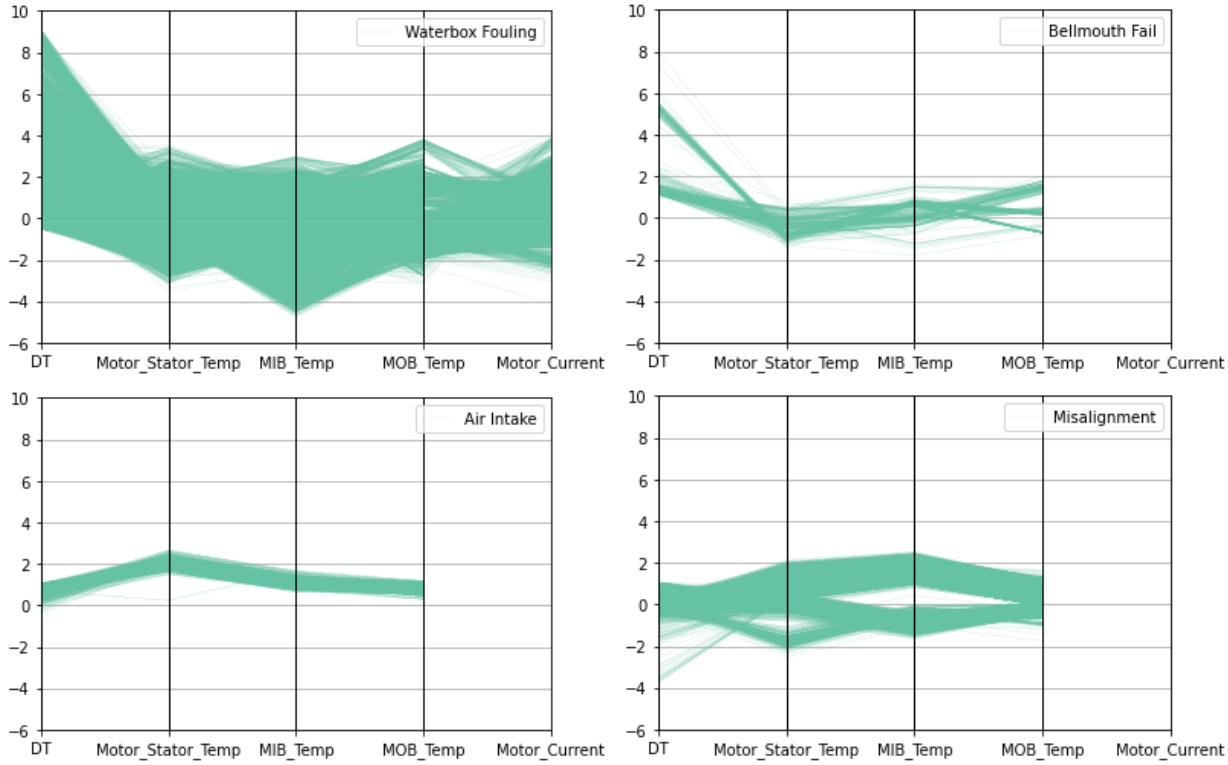

Figure 23. Parallel coordinate plots for the four considered failure states.

4.3 Margin Analysis

4.3.1 Margin Model for Air Intake and Misalignment

Given the provided context, both $\Xi^{obs-faulty}$ and $\Xi^{obs-healthy}$ data are available; hence, we have employed the density-based method described in Section 3.4 to estimate the $pdf^{healthy}(\xi^{obs})$ and $pdf^{faulty}(\xi^{obs})$. For this specific test case, we have considered a subset of the original data points contained in $\Xi^{obs-faulty}$ and $\Xi^{obs-healthy}$ over four monitored variables (i.e., DT, motor stator temperature, MIB temperature, and MOB temperature). We have considered a snapshot of the CWS system where an air intake instance was observed (between May 15 and July 8, 2008). By directly applying Eq. (12) for each ξ^{obs} it is possible to determine the corresponding margin value (see Figure 24). This plot shows the initial situation where the system is in a healthy state ($M^{sys} = 1$) and then the margin rapidly drops once it reaches the faulty condition. The two peaks that followed are generated during the repair time window.

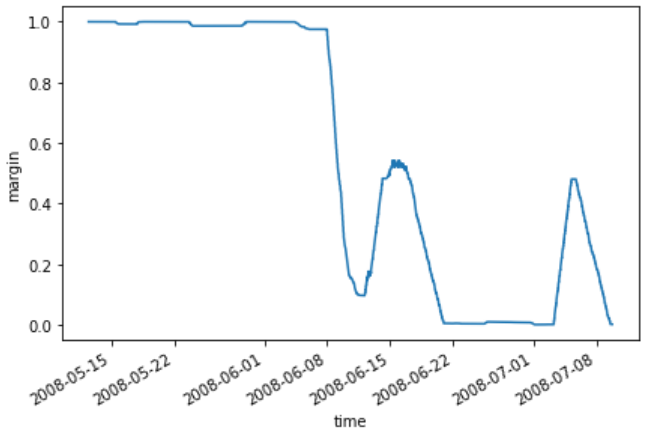

Figure 24. Graphical representation of margin for air-intake during an instance of air intake occurrence using density-based method.

An important element to highlight here is that the populations $\Xi^{obs-faulty}$ and $\Xi^{obs-healthy}$ for air intake are fairly separated as shown in Figure 21, Figure 20, and Figure 23. This allows us to assign a margin value $M^{sys} = 1$ when ξ^{obs} is located nearby the $\Xi^{obs-healthy}$ population and $M^{sys} = 0$ when ξ^{obs} is located nearby the $\Xi^{obs-faulty}$.

A similar situation can be generated for the misalignment failure mode. In this case however, the populations $\Xi^{obs-faulty}$ and $\Xi^{obs-healthy}$ are not completely separated as shown in Figure 21, Figure 20, and Figure 23. This is not an uncommon situation and might be caused by labeling process of the original data (healthy vs. misalignment). We have considered a snapshot of the CWS system where an air intake instance was observed (between April, 2008 and January, 2015). By directly applying Eq. (12) for each ξ^{obs} it is possible to determine the corresponding margin value (see Figure 25). This plot shows that the initial situation, where system is in a healthy state, is not actually characterized by $M^{sys} = .8$ (instead of $M^{sys} = 1$). This is caused by the fact that the distributions associated with the two populations $\Xi^{obs-healthy}$ and $\Xi^{obs-faulty}$ for the misalignment failure mode share some overlap (see also Figure 21). If the distributions of these two populations would not overlap, then $M^{sys} = 1$ when the system is in a healthy state.

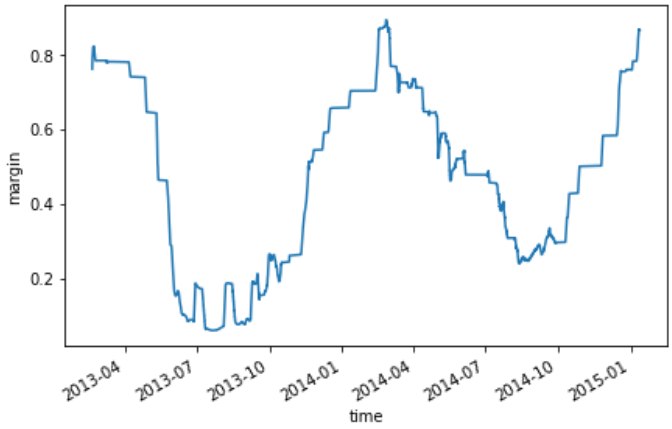

Figure 25. Graphical representation of margin for misalignment during an instance of misalignment occurrence.

4.3.2 Margin Model From ML Models

As indicated in (V. Agarwal, et al. 2021a, V. Agarwal, et al. 2021b), two ML models were generated to perform health and fault classification. Details of these two ML models are as follows:

- *Binary classifier*: this module is a XGBoost[3] binary classifier; for CWP data, it predicts whether the CWP is in normal operation or going through any degradation at the pump level, motor level or system level. The model is developed by considering time domain features extracted from vibration data along with the features extracted from monitoring data. Features like motor current and vibration data are not available before September 2017, and October 2019, respectively. The missing features are mapped with NaN values. The XGBoost model discards any feature with NaN value while training and making predictions. An example of prediction of the binary classifier model is shown in Figure 26.
- *Diagnostic model*: this module is a multiclass classifier; for CWP data, it predicts the type of fault that a CWP is currently going through. The model is developed by considering frequency domain features extracted from vibration data along with the features extracted from PI data. Features like Motor Current and Vibration data are not available before September 2017, and October 2019, respectively. The missing features are mapped with NaN values. The XGBoost Model discards any feature with NaN value while training and making predictions. An example of prediction of the diagnostic model is shown in Figure 27.

Time	Condition	Probability
2020-04-01	Unhealthy	0.873438

Figure 26. Example of prediction of the binary classifier model.

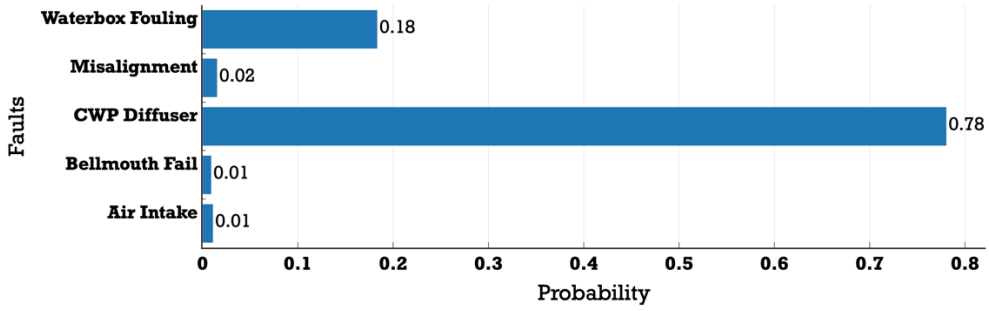

Figure 27. Example of prediction of the diagnostic model.

The outputs of these two ML models have been merged to assess margin for each failure mode using the set of Eq.s (13) through (15) indicated in Section 3.4. Figure 28 presents the margin associated with air intake using ML models; the same temporal profile can be compared with the one shown in Figure 24 where a density-based approach is applied to the same data set. This margin calculation has been applied to a subset of observation data ξ^{obs} which shows a transition from a healthy state to an air intake faulty state. This transition is captured in a margin sense by observing how CWS margin for air-intake drops from about 0.9 (system healthy) to 0.08 (system in an air-intake faulty state).

[3] Official website: https://xgboost.ai/

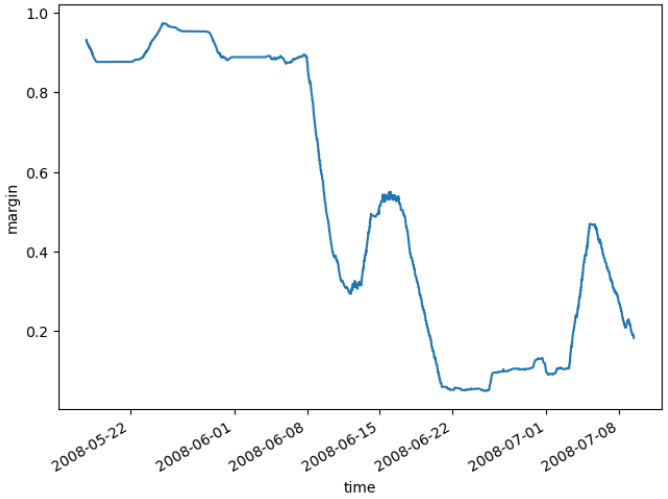

Figure 28. Graphical representation of margin for air-intake during an instance of air intake occurrence using ML models.

4.3.3 CWS Margin Model

The last analysis performed on the CWS data focused on tracking system health based on the full set of monitoring parameters. As indicated in Section 4.1, it is not uncommon that portions of the monitoring data elements might be missing in the dataset $\Xi^{obs-healthy}$ and $\Xi^{obs-faulty}$. This is not an uncommon scenario in an industrial context where a monitoring system might fail, or data might be corrupted.

In this respect we employed the distance-based method presented in Section 3.4. Based on the available dataset $\Xi^{obs-healthy}$ and $\Xi^{obs-faulty}$ (which include all the considered failure modes), the margin model described in Eq. (8) was employed to determine the margin associated with each failure mode. In order to address the scenario of missing data elements, we employed a modified version of the Euclidean distance; when calculating the distance between a pair of data elements, this formulation ignores feature coordinates with a missing value in either sample, and it scales up the weight of the remaining coordinates to compensate for the missing coordinates.

Figure 29 shows the temporal evolution of the margin associated with the three failure modes; the regions highlighted in green correspond to the times where such failures occurred. First, note that margin values reach a 0 value when actual failure occurs. Then, note how margin temporal profiles are characterized by fluctuations and periodic behaviors. While these fluctuations are relatively limited for air intake (bottom plot of Figure 29), they are more pronounced for the other failure modes. This is mostly driven by the fact that the population $\Xi^{obs-healthy}$ and $\Xi^{obs-faulty}$ for these failure modes are not completely separated as graphically shown in Figure 21.

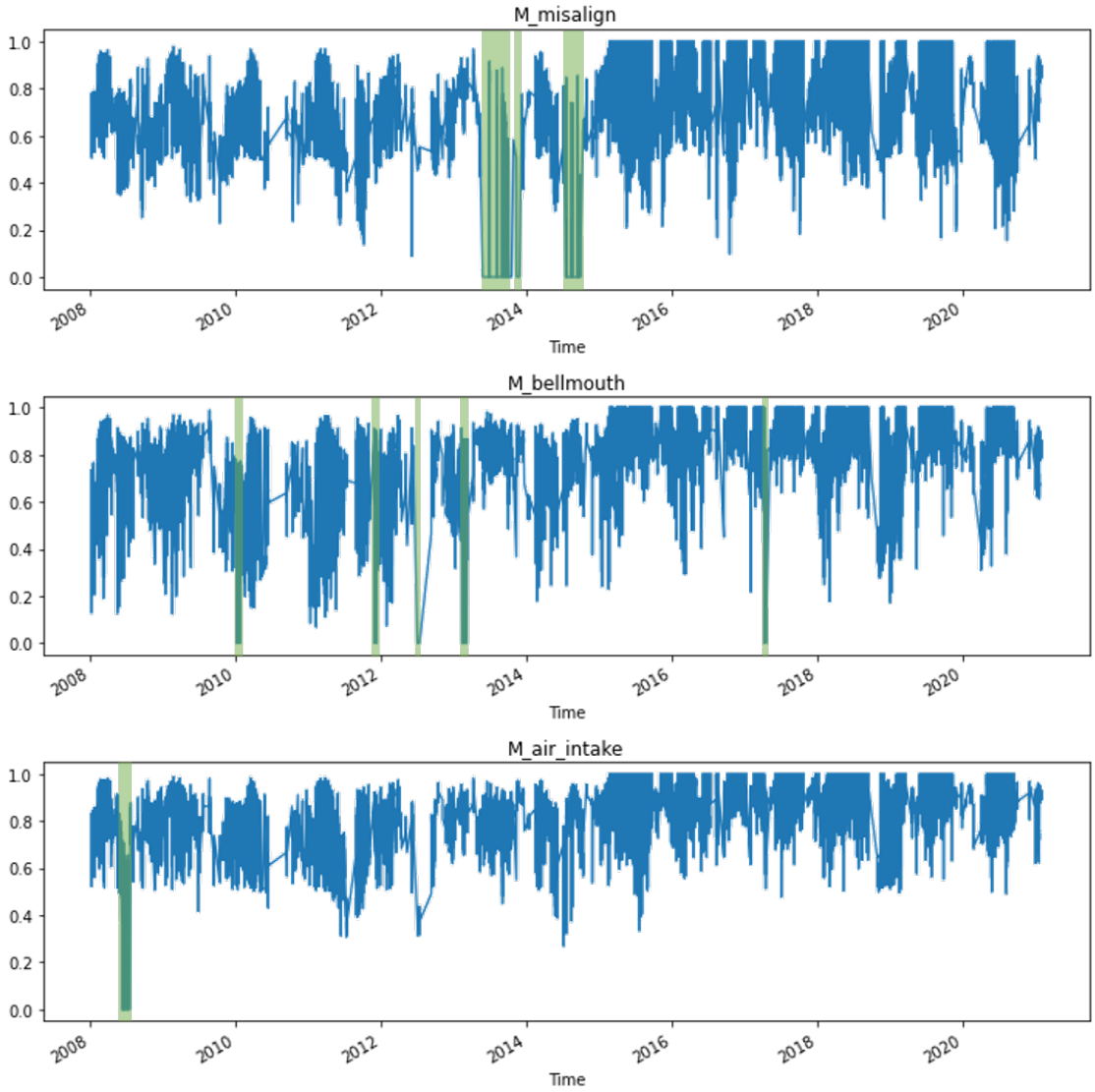

Figure 29. Temporal profile of margin associated with some failure modes of the CWS system.

4.4 RUL Estimation

In order to increase system reliability and safety and reduce O&M costs, nuclear power plants are moving from corrective and periodic maintenance to predictive maintenance strategies. RUL has been found to be a key risk indicator for predictive maintenance and is critical to operations and decision making. It indicates how long an asset can operate before it requires repair or replacement. Accurately predicting RUL can enable significant NPP improvement, since it can provide early warnings of failure to avoid unplanned downtime and economic losses. By taking RUL into account, engineers can develop a dynamic and optimized predictive maintenance strategy to improve operating efficiency with enhanced reliability and safety.

There are many approaches that are used to derive an estimate of RUL, and different researchers categorized RUL studies into several different categories (C. Okoh, et al. 2014). However, the techniques are generally divided into two main categories: physical-based and data-driven methods. Physical-based methods require modeling of the asset; however, model development is expensive and not always

achievable. Moreover, the NPP is a complex system that makes the modeling of degradation mechanisms a very complicated process. Data driven methods are more flexible and effective, and do not require an accurate dynamic model for the asset and its degradation process. They use ML and artificial intelligence (i.e., deep neural network, support vector machines, Bayesian networks) to learn the underlying degradation behaviors from historic data. However, the challenge of the data driven approach is the requirement for a training dataset; the data driven method used to estimate RUL depends on the kind of data available:

1. Reliability-based methods, such as hazard modeling and Bayesian techniques, require lifetime data or run-to-failure histories of assets
2. Supervised learning methods, such as neural networks, support vector machines and regression methods, require labeled RUL in a representative training dataset.
3. Time-series forecasting methods, such as autoregressive integrated moving average (ARIMA), Prophet Model, and Four Theta Model, can be used to estimate RUL when there are limited data and a known threshold value of a condition indicating failure of defects.

NPP operating data for various working conditions with different failure or degradation modes are often subject to export control for security reasons. Hence, it is difficult to acquire these historical data, making it even harder for researchers to develop physical based models, apply reliability-based approaches, or train supervised learning algorithms to accurately estimate RUL of assets. In this situation, time-series forecasting methods can be employed as a surrogate to estimate the RUL since they can be applied on limited historic data. They can also be treated as supervised learning methods once a labeled RUL training dataset is available, and some of the methods can also make use of past and future covariates to improve the estimation accuracy (J. Herzen, et al. 2022).

In this study, we start with limited historical vibration data for the CWS at a PSEG-owned plant (V. Agarwal, et al. 2021a, V. Agarwal, et al. 2021b). Accurately estimating the CWS RUL will result in significant economic benefits. In (V. Agarwal, et al. 2021b), the authors utilize a hazard model to estimate ongoing degradation without relying on any physical modeling. However, such methods need to assume a life distribution such as the Weibull distribution used by the authors and lifetime data. We have examined several time-series forecasting methods, such as ARIMA, Four Theta, deep neural network (e.g., LSTM, N-BEATS, and BATS), exponential smoothing, and Prophet for predictions of RUL. A python library Darts that contains all of these models is utilized to test and compare performance. What we have found is Prophet model (Taylor, S. J., Letham B. 2018) can be tuned to estimate the long-term (i.e., days and months) degradation behavior with limited data, and the rest of the models can only estimate the short-term (i.e., up to few hours) degradation behavior and then these models will start to deviate from validation data.

In Prophet model, the time series are decomposed into three main pieces (Taylor, S. J., Letham B. 2018):

$$V(t) = g(t) + s(t) + o(t) + \epsilon_t \tag{21}$$

where $g(t)$ is the trend function which models non-periodic changes in the value of the degradation data, $s(t)$ represents periodic changes (e.g., weekly/monthly/yearly seasonality), and $o(t)$ represents the effects of dynamic operations which occur on regular schedules. The white noise term ϵ_t, assumed to be normally distributed, represents the changes which are not accommodated by the model. Prophet model utilizes continuous piece-wise linear functions to model the trend, i.e., a combination of an offset and a growth rate. This allows the growth rate to change at different locations depending on the characteristics of the given time-series data. This results in an interpretable, yet non-linear form of the trend. In other words, the trend effect within a time window between two change points is given by the steady growth rate multiplied by the difference in time.

Prophet model incorporates trend changes by explicitly defining changepoints where the growth rate is allowed to change. This feature is very important when modeling the degradation process since the model allows users to directly specify the start time of aging as a changepoint and the time window that will be used to forecast the degradation behavior. Another important hyper-parameter is the changepoint prior scale that is used to control the flexibility of the trend, and in particular how much the trend changes at the trend

changepoints. In other words, small value of changepoint prior scale indicates small variance on the trend changes, while a large value indicates large variance on the trend changes; in the most extreme case the trend will end up capturing the seasonality too. In Figure 30, the long-term predication for the CWS degradation process is plotted with its variation on the trend predictions (i.e., the region shaded in blue represents the confidence bounds: 5th percentile to 95th percentile). We set the final trend segment to 20% of training data as observed from the measured data to capture the degradation trend and to avoid overfitting on a small number of aging points or underfitting on a large number of normal operation data. The changepoint prior scale is tuned to make the model better represent the degradation process. One can use the given failure threshold indicated by red horizontal line and the predictions to determine the RUL distribution as illustrated in Figure 30.

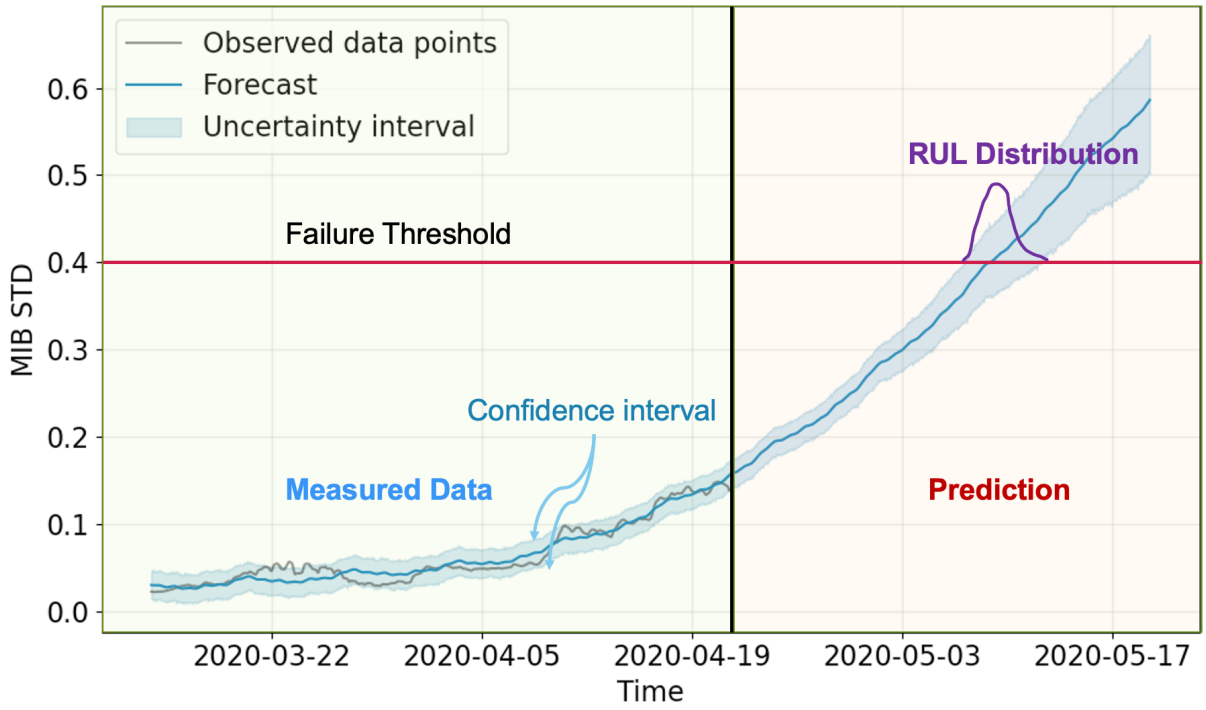

Figure 30. RUL estimation of Salem CWS based on vibration data using Prophet model.

The main advantage of using Prophet model is its ability to utilize piece-wise linear functions to capture the characteristic changes in trend. Moreover, as mentioned in (Taylor, Letham 2018), it can also integrate the effects of dynamic operations that occur on regular schedules in RUL estimation, which could greatly improve the accuracy in the estimation when there are large peaks or dips caused by the dynamic operations.

As mentioned in (Agarwal, et al. 2021b), the primary issue noted with the Salem CWS is fouling of the waterboxes by grass and debris. Fouling of the waterboxes typically occurs due to accumulation of grass/debris in the waterbox, resulting in condenser tube blockage and reduced circulator water flow. As reported in (V. Agarwal, et al. 2021b), waterbox fouling is typically identified via:

1. Motor current increase (also, though far less frequently, motor current decrease)
2. Inlet pressure increase
3. Waterbox DT increase
4. Condenser thermal performance loss

Once the run-to-failure data or lifetime data are recorded for above mentioned indicators, supervised learning algorithms can be used to predict the RUL and will be compared with the time-series forecasting method**.**

5. Decision Making

As indicated in Section 3, a margin-based reliability modeling approach is able to quantify asset health given available ER data and provide insights about the most critical assets that might negatively affect system operation (through the reliability measure RIM described in Section 2 and Eq. [3]). In Section 3.7, we have provided an example where we tracked the margin of a system composed of seven assets, and the RIM profile of each asset. In the same example we did not consider asset restoration once its performance was deemed unacceptable (e.g., when asset margin is approaching 0). In a predictive maintenance context, assets are not run until they fail; instead, maintenance operations are performed only when failure is approaching.

Hence, maintenance operations should be constantly prioritized and scheduled to guarantee system operation. This process requires an additional piece of information regarding the timing aspect associated with asset degradation. This information is captured by the concept of urgency, which is defined as the amount of time available between now and when restoration operations need to start to avoid asset failure (see Figure 31). From a practical standpoint, the asset urgency estimation requires two time values:

- Estimated failure time of the asset, which can be available from prognostic data (i.e., through RUL) or by measuring the temporal decline in asset margin (see [Mandelli, 2022]);
- Time required to restore asset health. If the restoration process requires the replacement of the asset, the time value can include the time to: obtain the new asset (procurement time), replace the old asset, and install the new asset. If the restoration process requires onsite activities (e.g., chemical treatment of corroded portions of the asset), the restoration time can include the time to: take the asset offline, perform the restoration activity, and place the asset back online.

At this point, we can select the most critical maintenance operations based on their urgency and the reliability importance of the assets by plotting all operations on an urgency vs. importance plot as indicated in Figure 32. Depending on the decision-making context, this 2D plot can be partitioned in multiple regions where the range of each dimension is divided into two or three intervals. The selection of the operations that should be performed to guarantee future system operation can be made by choosing the operations in selected partitions of the urgency vs. importance plot. As an example, for the case shown in Figure 32, the operations landing in the red, dark orange, and light orange sectors should be chosen as candidate assets that require maintenance attention.

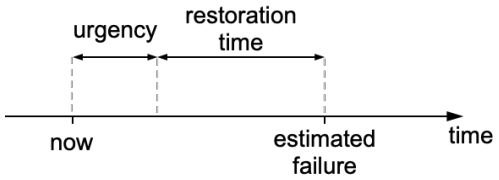

Figure 31. Graphical representation of urgency given estimated asset failure and required restoration time.

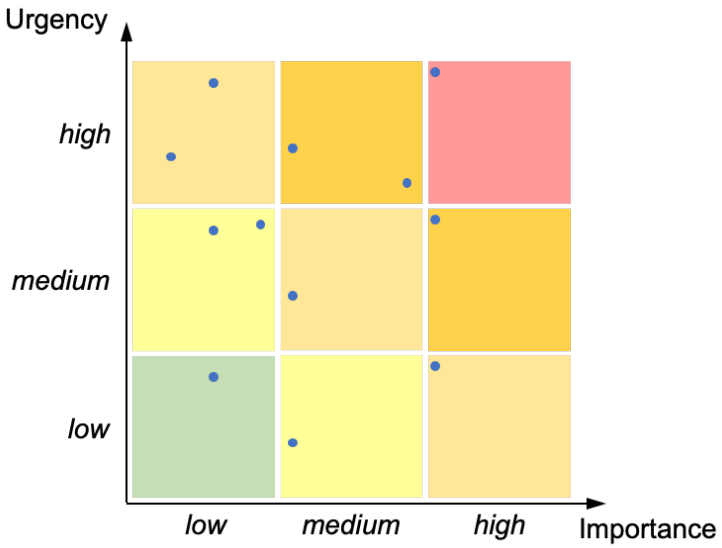

Figure 32. Selection of the most critical assets in an urgency-importance diagram.

Next, this set of candidate maintenance operations needs to be prioritized and scheduled. This task might include the fact that maintenance budget funds are limited and spread over multiple time windows (e.g., quarterly or during power plant outage), and maintenance activities can be performed on specific time windows (see reference [Wang, 2020] for more details). This can be accomplished using data-based optimization methods that are based on the knapsack model. Here, for each maintenance activity, an execution option is specified (i.e., a time window to perform such activity); each option is characterized by a risk factor which balances asset failure (e.g., likelihood of failure in that time window which is available from a margin analysis) and its consequences (e.g., in terms of loss of money which can be caused by power derate while the asset is being restored). Once all options have been set for all candidate maintenance activities, the optimization method based on the knapsack model will generate the optimal execution schedule (i.e., a specific single option for each maintenance activity) which satisfies the budget constraints and minimizes overall risk [Wang, 2020].

6. Conclusions

This paper has provided an alternative approach to perform system reliability modeling designed to directly employ available monitoring data to support decisions in a predictive maintenance context The starting point of our work is based on the objectives of reliability modeling: the assessment and management of system health by utilizing the integrated health information of all its assets.

We began by presenting a margin-based approach to assess health information of an asset which is based solely on current and historic monitoring data (e.g., condition-based, anomaly detection, diagnostic, and prognostic data). We have provided details on how heterogenous ER data elements are employed to assess the status of an asset through a margin value which is essentially an analytical measure of its health. We have shown how, depending on operational context of the asset (e.g., type of failure modes) and its available data, a margin value can be quantified using well known statistical and machine learning algorithms.

The assessment of system health is performed by propagating the margin values of the assets that support system function(s) through classical reliability models (e.g., FTs or reliability block diagrams). Such propagation is not performed through set theory-based rules, but through distance-based operations instead. This information can then be used to assess reliability importance of each asset in order to identify

the most critical assets. A margin-based approach directly addresses the limitations of classical reliability modeling approaches, and it provides a snapshot of system health given available monitoring data. However, we have indicated how classical and margin-based approaches provide identical results when MTTF value are provided for each asset. These two different approaches are designed to address different kind of decisions: classical reliability models support *static* decisions (e.g., set frequency of periodic maintenance or surveillance operations) based on past operational experience. A margin-based approach directly supports *dynamic* decisions where maintenance operations should be performed only when are necessary based on monitoring data (i.e., a predictive maintenance context). Note that the application of these two types of decisions (i.e., *static* and *dynamic*) is dictated by the degradation process under consideration. When asset failure occurs suddenly or monitoring system cannot capture asset degradation, then classical reliability approaches can be here used to set preventive maintenance and periodic surveillance frequencies. On the other hand, when asset progressively degrade and the installed monitoring system is able to capture degradation trend, then a predictive maintenance context that relies on a margin-based approach can be set.

We have provided a few examples to show how this process can be completed and the outcomes of such analysis not only in terms of system health but also in terms of the importance of each asset. The analysis of the CWS system of an existing power plant has provided insights on the operational context and the structure of real data. Developed statistical and machine learning methods were employed to assess system health through margin-based operations.

Lastly, this work complements (Mandelli, 2022), and it provides a more in-depth analysis of a margin-based reliability approach, and its direct application on a dataset generated by the monitoring system of the CWS system of an existing power plant. A margin-based interpretation of reliability transforms the concept from one that focuses on the probability of occurrence to one that focuses on assessing how far away (or close) an asset is to an unacceptable level of performance or failure. This transformation has the advantage that it provides a direct link between the asset/system health evaluation process and standard plant processes used to manage plant performance (e.g., the plant maintenance and budgeting processes). The transformation also places the question into a more familiar and readily understandable form for plant system engineers and decision makers (Xingang, 2021).

References

Agarwal, V. et al. (2021a). "Machine Learning and Economic Models to Enable Risk-Informed Condition Based Maintenance of a Nuclear Plant Asset," Idaho National Laboratory Technical Report, INL/EXT-21- 61984, Rev. 0. https://www.osti.gov/servlets/purl/1770866.

Agarwal, V. et al. (2021b). "Scalable Technologies Achieving Risk-Informed Condition-Based Predictive Maintenance Enhancing the Economic Performance of Operating Nuclear Power Plants," Idaho National Laboratory Technical Report, INL/EXT-21-64168.

ASME and ANS - American Society for Mechanical Engineers and the American Nuclear Society (2013). "Standard for Level 1/Large Early Release Frequency Probabilistic Risk Assessment of Nuclear Power Plant Applications," ASME/ANS RASb-2013, American Society for Mechanical Engineers and the American Nuclear Society.

Baraldi, P., F. Di Maio, P. Turati, E. Zio, (2015). "Robust Signal Reconstruction For Condition Monitoring of Industrial Components via a Modified Auto Associative Kernel Regression Method," Mechanical Systems and Signal Processing, vol.s 60-61, pp. 29-44.

Ferreira, C., and G. Gonçalves (2022). "Remaining Useful Life Prediction and Challenges: A Literature Review on the Use Of Machine Learning Methods," Journal of Manufacturing Systems, vol. 63, pp. 550-562. https://doi.org/10.1016/j.jmsy.2022.05.010.

Herzen, J. et al. (2022). "Darts: User-Friendly Modern Machine Learning for Time Series," Journal of Machine Learning Research, 23, 1-6.

Lee, J. C., N. J. McCormick (2011). *Risk And Safety Analysis of Nuclear Systems*. Wiley ed.

Luo Y., W. Zhang, Y. Fan, Y. Han, W. Li, E. Acheaw (2021). "Analysis of Vibration Characteristics of Centrifugal Pump Mechanical Seal under Wear and Damage Degree," Shock and Vibration, 2021. https://doi.org/10.1155/2021/6670741.

Mandelli, D., C. Wang, S. Hess (2022), "On the Language of Reliability: A System Engineer Perspective," Accepted for publication for Nuclear Technology.

Mohri, M., A. Rostamizadeh, A. Talwalkar (2012). *Foundations of Machine Learning*. The MIT Press.

Nassif, A. B., M. A. Talib, Q. Nasir, F. M. Dakalbab (2021). "Machine Learning for Anomaly Detection: A Systematic Review. IEEE Access, 9, 78658–78700. https://doi.org/10.1109/ACCESS.2021.3083060.

Okoh, C. et al. (2014), "Overview of Remaining Useful Life Prediction Techniques in Through-Life Engineering Services," Procedia CIRP 16, 158-163.

Rausand, M., A. Barros, A. Hoyland (2020). *System Reliability Theory: Models, Statistical Methods, and Applications*. Wiley ed.

Siu, N., D. Kelly (1998). "Bayesian Parameter Estimation in Probabilistic Risk Assessment," Reliability Engineering and System Safety, 62, pp. 89-116.

Taylor, S. J., B. Letham (2018). "Forecasting at scale," The American Statistician 72(1), 37-45.

Hastie, T., R. Tibshirani, J. Friedman (2001). *The Elements of Statistical Learning*. New York: Springer.

U.S. CFR - United States Code of Federal Regulations (2010) "Maintenance of Records, Making of Reports," 10 CFR 50.71, Section (h)(2), United States Code of Federal Regulations.

Wang, C., D. Mandelli, S. St. Germain, C. Smith, D. Morton, I Popova, S. Hess (2020). "Stochastic Optimization for Long Term Capital Structures, Systems, and Components Refurbishment and Replacement," Proceedings of the 2020 28th Conference on Nuclear Engineering Joint with the ASME 2020 Power Conference ICONE28-POWER2020.

Xingang, Z., J. Kim, K. Warns, X. Wang, P. Ramuhalli, S. Cetiner, H. G. Kang, M. Golay (2021). "Prognostics and Health Management in Nuclear Power Plants: An Updated Method-Centric Review with Special Focus on Data-Driven Methods," Frontiers in Energy Research, 9, 696785. https://doi.org/10.3389/fenrg.2021.696785.

Youngblood, R.W. (2001). "Risk Significance and Safety Significance," Reliability Engineering & System Safety, 73(2), 121–136. https://doi.org/10.1016/S0951-8320(01)00056-4.

Zhang, L., J. Lin, B. Liu, Z. Zhang, X. Yan and M. Wei (2019). "A Review on Deep Learning Applications in Prognostics and Health Management," in IEEE Access, vol. 7, pp. 162415-162438, doi: 10.1109/ACCESS.2019.2950985.